CHARLES UNIVERSITY

Faculty of Science

Study programme: Clinical and Toxicological Analysis

Bc. Barbora Judita Kasperová

NEUROPROTECTIVE EFFECTS OF FOOD INTAKE REGULATING PEPTIDES *IN VITRO* AND *IN VIVO*

Neuroprotektivní účinky peptidů ovlivňujících příjem potravy *in vitro* a *in vivo*

Diploma thesis

Supervisor: RNDr. Lenka Maletínská, CSc.

Prague 2018

Prohlášení

Prohlašuji, že jsem tuto závěrečnou práci zpracovala samostatně a že jsem uvedla všechny použité informační zdroje a literaturu. Tato práce ani její podstatná část nebyla předložena k získání jiného nebo stejného akademického titulu.

Jsem si vědom toho, že případné využití výsledků, získaných v této práci, mimo Univerzitu Karlovu je možné pouze po písemném souhlasu této univerzity.

V Praze dne

PODĚKOVÁNÍ

Ráda bych poděkovala své školitelce RNDr. Lence Maletínské, CSc. za vedení a pomoc při konzultacích k experimentální činnosti a při psaní mé diplomové práce.

Mé poděkování dále patří Mgr. Andree Popelové, Ph.D a Ing. Blance Železné, CSc. za přínosné rady a trpělivost při experimentální činnosti a psaní mé diplomové práce. Zároveň bych ráda poděkovala celému kolektivu ze skupiny Antiobezitní peptidy, ÚOCHB AV ČR, v.v.i. Zejména RNDr. Martině Holubové, Ph.D., RNDr. Veronice Pražienkové, Ph.D. a Ing. Janě Zemenové za neutuchající motivaci, cenné rady a vřelou podporu.

V neposlední řadě bych ráda poděkovala celé své rodině a nejbližším přátelům.

ABSTRACT

Nowadays, Alzheimer's disease (AD) is one of the most serious health problems among elder. To this day, pathogenesis of AD is still unknown and therefore no effective treatment has been found. AD is characterized by neuropathological features, the formation of extracellular senile plaques of amyloid β and intracellular neurofibrillary tangles of Tau protein. Numerous experimental studies have confirmed that metabolic disorders such as type 2 diabetes mellitus or obesity contribute significantly to the development of cognitive impairment and therefore the development of AD.

In this diploma thesis, the potential neuroprotective effect of peptides regulating food intake was investigated in *in vitro* and *in vivo* experiments.

The potential neuroprotective effect of liraglutide, a glucagon-like peptide-1 analog used as a type 2 diabetes mellitus treatment, a prolactin-releasing peptide (PrRP) and its palmitoylated analog, palm^{11}-PrRP31, was investigated on SH-SY5Y cell line. The peptides were used as a pretreatment on SH-SY5Y cells in methylglyoxal-induced cytotoxicity. It has been proven that the peptides themselves are not toxic and do not significantly reduce the viability of SH-SY5Y cells. The tested peptides showed prophylactic effects against cytotoxicity and apoptosis induced by toxic methylglyoxal.

Furthermore, the neuroprotective effect of the palmitoylated analog palm^{11}-PrRP31 on the Tau protein hyperphosphorylation and the activation of the neurogenesis markers in the hippocampi of the THY-Tau22, mice overexpressing mutant human Tau protein, have been observed. After 2 months of treatment with palm^{11}-PrRP31 analog, there was a significant attenuation of Tau protein hyperphosphorylation at epitopes Thr231, and non-significant reduction at Ser202 and Thr205. No significant difference was observed in neurogenesis markers, such as doublecortin and brain-derived neurotrophic factor (BDNF).

A neuroprotective effect of the palmitoylated analog PrRP31 on insulin signaling pathway, Tau phosphorylation and the activation of the neurogenesis markers in hippocampi of Koletsky rats (SHROB), a model of metabolic syndrome, have been observed. After 3-week-long intraperitoneal (IP) administration of palm^{11}-PrRP31, significant decrease in phosphorylation of Tau protein at epitopes Ser396 and Ser404 was observed. On the other hand, non-significant decrease was observed at Thr231

epitope. Furthermore, a significant decrease in cdk-5 activation was observed. Cdk-5 is one of the main kinases affecting Tau protein phosphorylation. A significant increase in activation of marker of synaptic density, postsynaptic density protein 95 (PSD95), was observed. No significant changes were observed in insulin signaling pathway.

In conclusion, analog palm^{11}-PrRP31 is proposed as a potential neuroprotective agent for further studies of its mechanism.

KEY WORDS

Tau (hyper)phosphorylation

Alzheimer's disease

SH-SY5Y cells

THY-Tau22 mice

Koletsky rats

Prolactin-releasing peptide

Liraglutide

Methylglyoxal

Apoptosis

Neurogenesis

Insulin signaling pathway

ABSTRAKT

Alzheimerova nemoc (AN) je jedním z nejzávažnějších onemocnění současnosti. Patogeneze AN je dosud neznámá, a tudíž neexistuje účinná léčba. AN je charakterizována dvěma neuropatologickými znaky, a to tvorbou extracelulárních senilních plaků amyloidního β peptidů a intracelulárních neurofibrilárních spletí proteinu Tau. Mnohé experimentální studie potvrdily, že metabolické poruchy jako je diabetes mellitus 2. typu (DM2T) či obezita výrazně přispívají právě k rozvoji kognitivních poruch a tedy i k rozvoji AN.

V této diplomové práci byl zkoumán potenciální neuroprotektivní vliv peptidů ovlivňujících příjem potravy a to jak v *in vitro* experimentech, tak *in vivo*.

Jako první byl zkoumán potenciální neuroprotektivní vliv liraglutidu, analogu glukagonu podobného peptidu 1 užívaného jako léku proti DM2T, peptidu uvolňujícího prolaktin a jeho pamitoylovaného analogu palm^{11}-PrRP31 po působení toxického methylglyoxalu na buněčnou linii SH-SY5Y. Bylo prokázano, že peptidy samotné nejsou toxické a signifikantně nesnižují viabilitu SH-SY5Y buněk. Testované peptidy vykazovaly preventivní účinky proti cytotoxicitě a buněčné smrti indukované toxickým methylglyoxalem.

Dále byl sledován neuroprotektivní účinek palm^{11}-PrRP31 na hyperfosforylaci proteinu Tau a aktivaci markerů neurogeneze v hipokampech THY-Tau22 myší se zvýšenou expresí mutovaného lidského proteinu Tau. Po 2 měsíčním působení palm^{11}-PrRP31 došlo k signifikantnímu snížení fosforylace proteinu Tau na Thr231 a nesignifikantnímu snížení fosforylace Ser202 a Thr205. Žádný signifikantní rozdíl nebyl pozorován u markerů neurogeneze, jako například BDNF a doublecortin.

Neuroprotektivní účinek palmitoylovaného analogu PrRP31 na inzulínovou signalizační kaskádu, hyperfosforylaci proteinuTau a aktivaci markerů neurogeneze byl sledován také v hipokampech Koletského potkanů (SHROB), kteří trpí metabolickým syndromem. Po 3 tydenním působení palmitoylovaného analogu palm^{11}-PrRP31 došlo k signifikantnímu snížení fosforylace proteinu Tau na epitopech Ser396 a Ser404. K nesignifikantnímu snížení fosforylace došlo na Thr231. Dále bylo pozorováno signifikantní snížení cyklin-dependentní kinasy cdk-5, která přímo ovlivňuje fosforylaci proteinu Tau. A také došlo k signifikantnímu zvýšení proteinu post-synaptické denzity PSD95, který ovlivňuje synaptickou plasticitu. Žádný signifikantní rozdíl nebyl shledán

v inzulínové signalizační kaskádě.

Analog palm^{11}-PrRP31 je potenciální neuroprotektivní látkou vhodnou ke dalšímu studiu mechanismu účinku.

KLÍČOVÁ SLOVA

(Hyper)fosforylace proteinu Tau

Alzheimerova nemoc

SH-SY5Y buňky

THY-Tau22 myši

Koletského potkani

Peptid uvolňující prolaktin

Liraglutid

Methylglyoxal

Apoptóza

Neurogeneze

Inzulínová signalizační kaskády

CONTENTS

ABBREVIATIONS

α-GAPDH – α-glyceraldehyde 3-phosphate dihydrogenase

AD – Alzheimer's disease

Akt – protein kinase B

AN – Alzheimerova nemoc

ANOVA – analysis of variance

APP - amyloid precursor protein

ARC – *arcuate nucleus*

Aβ – amyloid-β peptide

BBB – blood-brain barrier

BDNF – brain-derived neurotrophic factor

BM – Barnes maze

BSA – bovine serum albumin

CA1 – *cornu ammonis* 1

cdk-5 - cyclin-dependent kinase 5

CNS – central nervous system

db - diabetic

DMEM – Dulbecco´s modified eagles medium

DMN – dorsomedial hypotalamic nucleus

DMSO – dimethyl sulfoxide

DM2T – diabetes mellitus 2. typu

fa – fatty gene

FBS – fetal bovine serum

GLP-1 – glucagon-like peptide 1

GPR10 - G-protein-coupled receptor 10

GSK-3β - glycogen synthase kinase 3β

INT – iodonitrotetrazolium violet

IP – intraperitoneal

IR – insulin receptor

IRS1- insulin receptor substrate 1

JNK – c-Jun N-terminal kinase

KO – knock out

LDH – lactate dehydrogenase

MG - methylglyoxal

MSG – monosodium glutamate

MTT - 3-(4,5-dimethylthiazol-2-yl)-2,5-diphenyltetrazolium bromide

MWM – Morris water maze

NADPH – nicotinamide adenine dinucleotid phosphate

NGF – nerve growth factor

NTF - neurofibrillary tangles

NTS – *nucleus tractus solitarius*

OFM – open field maze

PBS – phosphate-buffered saline

PDK-1 – 3-phosphoinositide-dependent protein kinase 1

PI3K – phosphoinositide 3 kinase

PP2A – protein phosphatase 2A

PrRP - prolactin-releasing peptide

PS1 – presenilin-1

PSD95 – postsynaptic density protein 95

SDS – sodium dodecyl sulphate

SEM – standard error of mean

SHR – spontaneously hypertensive rat

SHROB - spontaneously hypertensive obese rat

sub - subunit

TBS – Tris-buffered saline

Tris – Trizma base

T2DM – type 2 diabetes mellitus

WAT – subcutaneous and visceral fat

WT – wild-type

1 INTRODUCTION

Alzheimers disease is one of the most serious neurodegenerative disease in the world. AD is characterized by intracellular neurofibrillary tangles by hyperphosphorylated Tau protein and extracellular β-amyloid plaques .

By 2010, more than 35 million people have been affected by AD worldwide and over the next 35 years this number is likely to rise to 115 million patients. For this reason, AD may be considered as a pandemic of the 21st century. The mechanism of AD still remains unknown. Up to this day, the only diagnosis of AD is postmortem brain autopsy [1,2].

The aim of this diploma thesis is to investigate the possible neuroprotective efffects of peptides tested *in vitro* using neuroblastoma SH-SY5Y cell line. And possible neuroprotective effects of novel analog palm^{11}-PrRP31 *in vivo* using mice model of tauopathy, THY-Tau22 mice, and rat model of metabolic syndrome, Koletsky rats.

Aims of thesis

1. *In vitro* characterization of potent neuroprotective properties of PrRP analog and liraglutide as its comparator on SH-SY5Y cells treated with cytotoxic methylglyoxal
2. Characterization of the long-term effect of PrRP analog on metabolic parameters and hyperphosphorylation of overexpressed human pathological Tau protein in hippocampi of THY-Tau22 mice, model of Tau pathology
3. Investigation of the effect of PrRP analog on pathological phosphorylation of Tau protein in hippocampi of spontaneously hypertensive obese Koletsky rats (SHROB), model of metabolic syndrome

2 STATE OF ART

2.1 Alzheimer's disease

Alzheimer's disease (AD) is one of the most serious world health problems and the most prevalent form of dementia among older adults. Dementia is a brain disorder causing the loss of cognitive functions and behavioral abilities. AD accounts for 60-80% of dementia cases. To date, no biomarkers are known to diagnose AD in patients, the only certain diagnosis is postmortem autopsy [3].

AD as a progressive neurodegenerative disorder causes irreversible brain damage, cell death which leads to significant loss of neurons and major loss of synaptic connections. Neuropathologically, AD is characterized by presence of extracellular senile plaques of amyloid-β peptide (Aβ) and intracellular neurofibrillary tangles (NTF) of hyperphosphorylated Tau protein. First region of the brain affected by AD is hippocampus that is a part of the limbic system and is associated with memory and spatial navigation.

Hippocampus is a part of the cerebrum, which is the largest and the most developed part of brain [4,5].

Initial symptoms of AD lead to decline in cognitive abilities, such as memory loss, confusion with time or place, worsened ability to remember new information, as well as problems with speaking. AD leads to behavioral changes and changes in personality and mood, including depression, apathy and increased anxiety. According to statistics, AD is 5th cause of death for people aged 65 and older [4,6].

Main risk factor of AD is considered to be aging. Recently, obesity, insulin resistance, type 2 diabetes mellitus (T2DM), or high blood pressure, diseases which are part of the metabolic syndrome, were associated with the increased risk of AD development. Several experimental and epidemiological studies have shown that there are many similarities between AD and T2DM, such as impaired insulin signaling pathway [1-3]. Therefore, Suzanne M. de la Monte proposed „type 3 diabetes“ as a new term for AD [7].

2.1.1 Discovery of AD

AD was first descired by a Bavarian psychiatrist, Alois Alzheimer, who observed the main neuropathological changes in the brain of 50-year-old woman

Auguste Deter, who had an early-onset dementia with sleep disorders, memory loss, progressive confusion and aggresiveness. After her death in 1906, Alois Alzheimer observed histological alterations over the cerebral cortex in her brain of yet-unnamed disease. Autopsy of Auguste Deter's brain showed athrophied brain cells and shrinkage of the cerebral cortex. In 1910, Alzheimer's colleague, Emil Kraepelin, proposed the term Alzheimer's disease [8].

2.2 Major hallmarks of Alzheimer's disease

Two major histopathological hallmarks of AD are NFT accumulated inside neurons and senile plaques outside neurons in the brain (Fig. 1).

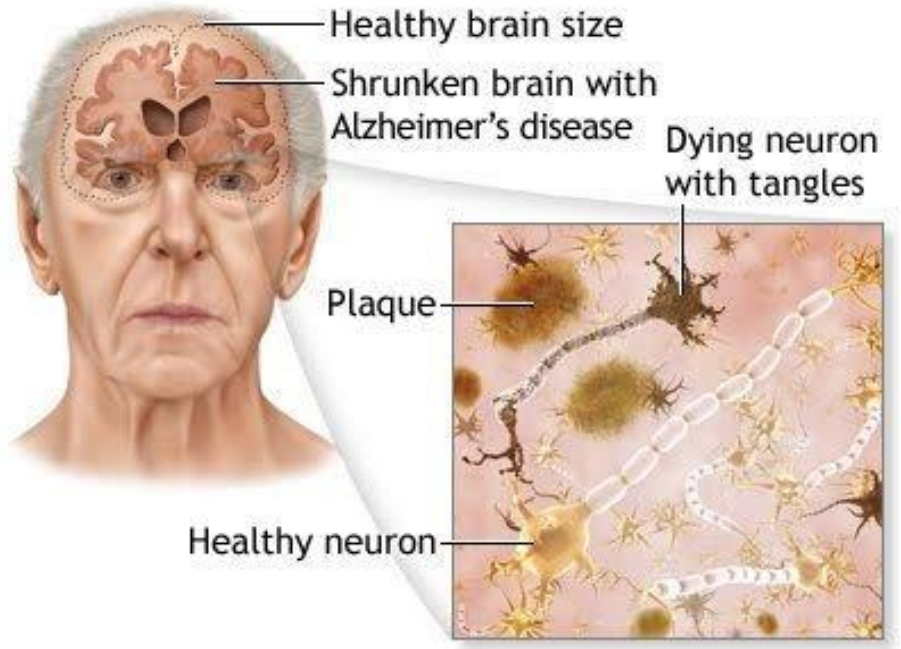

Fig. 1 Two major hallmarks of AD [9]

Intracellular NFT and extracellular senile plaques

2.2.1 Senile plaques and amyloid-β peptide

Senile plaques neuropathologically characterize AD. Senile plaques are extracellular aggregates composed of Aβ oligomers. Aβ is produced by the proteolytic cleavage of amyloid precursor protein (APP) and is identified as a 42 –43 amino acids peptide.

APP is a transmembrane protein which is present in the central nervous system

(CNS) and also in the periphery nervous system. Primary function of APP is not known, but it has positive effect on neural activity and memory in CNS. [10,11] Under normal physiological conditions, APP is cleaved by α-secretase into soluble peptide fragments. Pathophysiologically, APP is cleaved by β-secretase and γ-secretase which leads to formation of neurotoxic Aβ peptides. These chains polymerize and form insoluble extracellular senile plaques. Furthermore, Aβ promotes tau hyperphosphorylation and NTF pathology. Their neurotoxic effects contribute to synaptic dysfunction, cell death and chronic oxidative stress [12,13].

2.2.2 Neurofibrillary tangles

Intraneuronal neurofibrillary tangles formed by hyperphosphorylated Tau protein are another main histopathological hallmark of AD. Hyperphosphorylation of Tau protein leads to accumulation and fibril aggregation of abnormally phosphorylated Tau protein into insoluble structures. These fibril structures form NTF, particularly in the hippocampus.

In a brain which is affected by AD, Tau protein is phosphorylated three to four times more than in a healthy human brain [14,15].

2.2.3 Tau protein and its phosphorylation

Tau protein, as a part of microtubule associated proteins, plays an important role in stabilization of microtubule assembly in the cytoskeleton of neurons. Tau protein is predominantly expressed in axons in CNS, at lower levels in peripheral tissues (heart, muscles, kidneys). Tau protein is a heat-stable and highly soluble protein. The human Tau gene is located on chromosome 17q21 and contains 16 exons. Alternative splicing of exons 2, 3 and 10 allows six different isoforms of Tau protein. The expression of different isoforms of Tau protein is characteristic during brain development. Microtubule-binding domains are located in C-terminal part of Tau protein. Three isoforms of Tau have 3 microtubule-binding domains (isoforms without exon 10, Tau3R) and three isoforms have 4 microtubule-binding domains (isoforms including exon 10, Tau4R).

The most important post-translation modification of Tau protein is phosphorylation which regulates its binding and polymerizing activities.

As shown in Fig. 2, epitopes like Thr17, Tyr19 and Ser195 are physiologically phosphorylated in the normal brain. Other hydroxyl containing amino acids such as Ser202, Thr205 or Ser396 are phosphorylated in both, the normal and the AD brain. And epitopes of Tau protein such as Tyr18, Thr71 and Ser113 are phosphorylated in the AD brain. Phosphorylation on these epitopes of Tau protein promotes aggregation of Tau protein and inability to bind to microtubules.

Tau protein can be phosphorylated at multiple epitopes by various kinases. In particular, serine, threonine and tyrosine based epitopes can be phosphorylated. Kinases selectively phosphorylate these three amino acids on their hydroxy groups [15-17].

Numerous kinases and phosphatases regulate phosphorylation of Tau protein. The most important kinases are GSK-3β (glycogen synthase kinase 3β), cdk-5 (cyclin-dependent kinase 5) and JNK (c-Jun N-terminal kinase).

Cdk-5 is expressed in numerous tissues, highly in post-mitotic neurons and regulates many neuronal functions, including neuronal migration, synaptic activities or neuronal death [18]. Cdk-5 is involved in abnormal phosphorylation in the brain affected by AD. Hyperactivation of cdk-5 results in hyperphosphorylation of Tau protein with subsequent aggregation into microfilaments and NFT [19].

GSK-3β is the major regulator of adult hippocampal neurogenesis. It is multifunctional kinase that participates in the energetic metabolism, cell cycle and is part of many signaling pathways. GSK-3β is highly expressed in neurons in the brain, it is necessary for the formation of synapses and prolongation of dendrites. GSK-3β participates in insulin signaling pathway and is major Tau kinase which regulates Tau phosphorylation [20]. GSK-3β is a potential link between AD and T2DM. Ser9 phosphorylation regulates kinase activity of GSK-3β. Decreased levels of phosphorylation at epitope Ser9 activate kinase activity of GSK-3β toward Tau protein which leads to its pathological phosphorylation [21,22]. The level of GSK-3β is elevated in the brain affected by AD [23]. GSK-3β is also part of the regulation of glucose homeostasis [24].

Major Tau phosphatase that dephosphorylates Tau protein is protein phosphatase 2A (PP2A) [25].

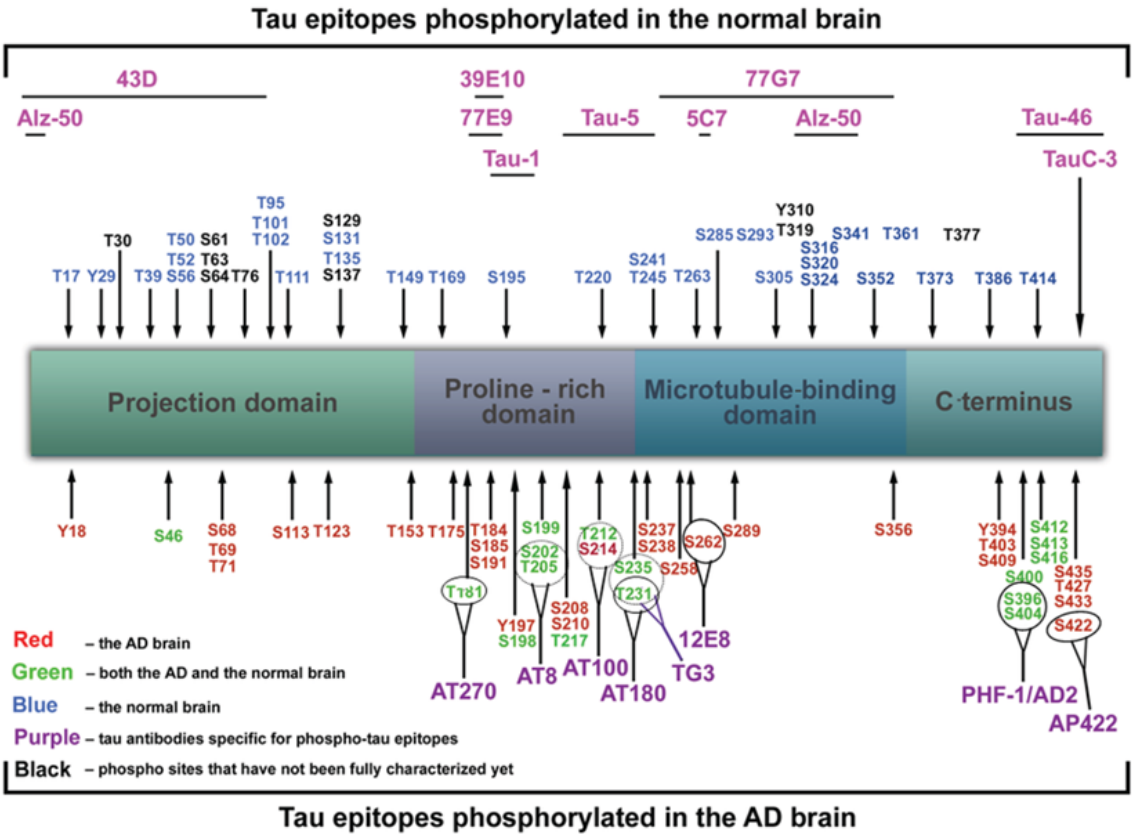

Fig. 2 Phosphorylation sites on Tau protein [17]

2.4 Type-2 diabetes mellitus

T2DM is one of the most common age-dependent metabolic disorders. T2DM is associated with high blood pressure, high level of cholesterol and cardiovascular diseases. Obesity is one of the main risk factors of T2DM development.

The main cause of T2DM is insulin resistance due to an imbalance between insulin secretion and its utilization in glucose metabolism. Inability of insulin receptors to respond to a changing level of insulin leads to their resistance to insulin. Inadequate insulin secretion leads to hyperinsulinemia and an impaired response to insulin leads to hyperglycemia, increased level of glucose in the blood. Hyperinsulinemia and hyperglycemia contribute to other serious health complications such as stroke or neuropathy [2,26,27].

2.5 Insulin and insulin signaling pathway

Hormone insulin is produced by β-cells of pancreas and passes to CNS via blood-brain barrier (BBB). The most insulin receptors in CNS were found in the cortex,

hypothalamus and hippocampus. As a major hormone regulating energy homeostasis, insulin is involved in glucose and lipids metabolism.

Physiologically, after the binding of insulin to insulin receptors (IR), insulin stimulates their autophosphorylation of their tyrosine residues.

The IR tyrosine kinase phosphorylates insulin receptor 1 (IRS1) which activates phosphorylation of phosphoinositide 3 kinase (PI3K) regulatory subunit p85 which further phosphorylates 3-phosphoinositide-dependent protein kinase (PDK-1) at Ser241 and activates protein kinase B (Akt) at Thr308 and Ser473. Once activated, Akt phosphorylates GSK-3β at Ser9 in the N-terminal part which inhibits the kinase activity of GSK-3β towards Tau [26,28].

2.6 Neuroprotective effect of food intake regulating peptides

2.6.1 Glucagon-like peptide 1

Glucagon-like peptide 1 (GLP-1) is produced by posttranslation modification from proglucagon gene which is produced in the brain, pancreas and intestine. GLP-1 is incretin hormone consisting of 31 amino acids and binds to GLP-1 receptor. GLP-1 receptors are found in the human brain, as well as in the brain of rodents.

GLP-1 is splitted from proglucagon and secreted by intestinal enteroendocrine L-cells. Intestinal enteroendocrine L-cells are found in the distal ileum, less in the duodenum and jejunum in the small intestine.

As a signaling peptide, GLP-1 has a lot of important physiological properties. L-cells secrete GLP-1 when glucose level in the blood is increased. GLP-1 is released in response to food intake and lowers blood glucose by stimulating insulin secretion and by inhibiting glucagon secretion in pancreas.

Besides of stimulation of insulin secretion, neuroprotective properties of GLP-1 were described. GLP-1 plays important role in the brain and its receptors are located in neurons. Dr. Christian Hölscher described that GLP-1 protects neurons from neurotoxicity and apoptosis [29]. The incretins are capable of reversing the damage that Aβ has on synaptic plasticity and reducing other AD degenerative processes.

2.6.2 Liraglutide

Naturally occuring incretins, such as GLP-1, have very short half-life in circulation. Therefore, their long-lasting analogs such as liraglutide have been invented.

Liraglutide is a stable and long-acting derivate of the gut hormone GLP-1. As shown in Fig. 3, its structure is slightly modified by attaching palmitic acid at Lys16 and substituting Lys34 by Arg. Due to modification, liraglutide has 10-14 hours longer half-life than GLP-1. Lipidization allows liraglutide non-covalent binding to plasma proteins.

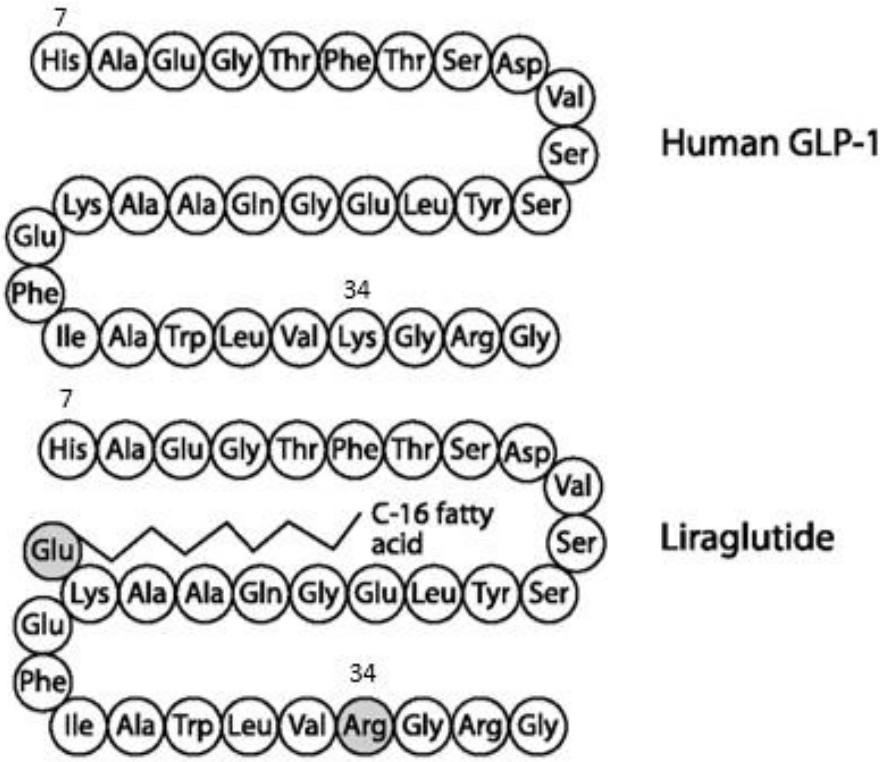

Fig. 3 Structure of human GLP-1 (upper panel) and analog of GLP-1, liraglutide (lower panel)[30]

Liraglutide is a first-choice drug in the treatment of T2DM. Recently, it was approved as a anti-obesity drug by U.S. Food and Drug Administration. Liraglutide is marketed by Novo Nordisk under brand name Victoza [31].

Liraglutide has also neuroprotective properties. Neuroprotective effects were

examined in various rodent models. For example McClean et al. described spatial memory improvement in water maze and object recognition tasks after IP administration of liraglutide. Increased levels of doublecortin and synaptophysin in APP/PS1 mice were also found, same as reduced number of Aβ plaques counted in the cortex in the brains of APP/PS1 mice [32].

2.6.3 Prolactin-releasing peptide

Prolactin-releasing peptide (PrRP) was discovered as an endogenous ligand of an orphan human G-protein-coupled receptor GPR10 (in rats UHR-1), isolated from mammalian hypothalamus using reverse pharmacology. PrRP is an anorexigenic neuropeptide belonging to the group of RF-amide neuropeptides containing arginine and phenylalanine at their C-terminus [33,34]. There are two biologically active isoforms of either 20(PrRP20) or 31 (PrRP31) amino acids containing an identical C-terminal sequence that is crucial for biological activity of PrRP (Fig. 4). PrRP20 and PrRP31 are formed from human precursor proPrRP consisting of 87 amino acids [35].

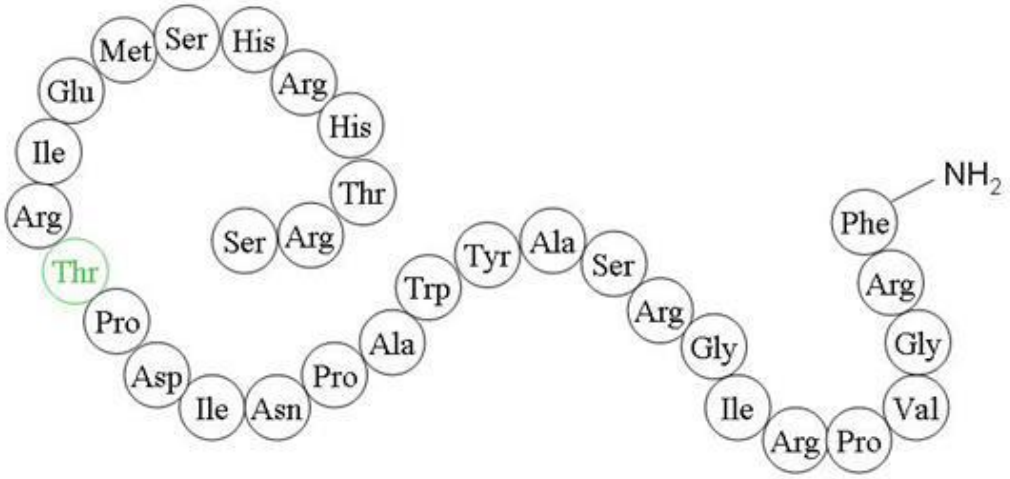

Fig. 4 Structure of human PrRP31 and PrRP20

The beginning of PrRP20 is marked with the green threonine

PrRP mRNA is expressed in neurons, primarily in the *nucleus tractus solitarius* (NTS) in the brainstem, lateral reticular nucleus of medulla oblongata, the ventrolateral medulla and the dorsomedial hypothalamic nucleus (DMN) in hypothalamus, less in

amygdala and anterior and posterior lobes of the pituitary gland. PrRP also occurs in pancreas, testicles and placenta in lower concentrations [36,37].

The receptor for PrRP, GPR10, consists of 369 amino acids and belongs to a large family of G-protein-coupled receptors that exhibit similar structural properties such as 7 hydrophobic transmembrane segments. Its structure is the closest to neuropeptide Y receptor (homology from 31% overall and 46% in transmembrane regions). It is possible that these receptors developed from one original receptor [38].

GPR10 occurs in CNS and peripheral tissues. GPR10 is located in the CNS at multiple sites, such as in paraventricular nucleus, periventricular nucleus, DMN and ventromedial core, in the anterior pituitary lobe, amygdala, in the post-cerebral artery and NTS. In peripheral tissues, GPR10 receptor mRNA was found only in the adrenal gland. In females, there is a higher number of receptors than in males [38-40].

PrRP has many physiological functions in human body. Initially, PrRP was proposed to stimulate the secretion of prolactin in *in vitro* study using RC-4B/C pituitary cell line. The secretion of prolactin was questioned and currently it is known that effect of prolactin secretion mediated by PrRP is not considered as its function. This fact was proved in various *in vivo* studies .

Because of the expression of mRNA in the brain areas regulating food intake, it was suggested that PrRP is involved in food intake regulation [35,41]. These findings were proven in several studies. showing anorexigenic effect after central administration of PrRP31 in rats [42]. The regulating function in food intake of PrRP was supported by the findings in GPR10 knockout (KO) mice study [43], where higher body were observed in GPR10 KO.

Naturally occuring PrRP is not able to cross BBB and reach the brain where it exerts its anorexigenic and potentially neuroprotective properties. Therefore, a new palmitoylated analog of PrRP31, palm11-PrRP31, was designed and synthesised in our laboratory. Palmitoylation resulted in increased stability in blood plasma, and moreover enabled the penetration through BBB. Thus, palm11-PrRP31 can be administred peripherally [44].

2.7 *In vitro* models for testing of neurodegeneration/neuroprotection

2.7.1 SH-SY5Y

SK-N-SH, a parental cell line of SH-SY5Y cells, originates from a bone marrow biopsy that contains epithelial and neuroblast cells. SH-SY5Y cell line has stable karyotype.

Neuroblastoma cell line SH-SY5Y is used in neurobiology and the neurosciences experiments for its differentiation from a neuroblastoma cells into mature neurons to study nerve cell metabolism and apoptosis. SH-SY5Y cells are frequently used in scientific research of Parkinson's disease, AD and viral pathogenesis [45,46].

SH-SY5Y cells were used in methylglyoxal-induced toxicity study to determine neuroprotective properties of liraglutide, by Sharma et al. [45].

2.7.2 PC12

The PC12 cell line was derived from pheochromocytoma, neuroendocrine rat tumor arising from the adrenal medulla. PC12 cells have polygonal shape and stable genotype and fenotype growing in small clumps.

PC12 cells are sensitive to nerve growth factor (NGF) protein. NGF-treated cells cease multiplication and form synapses, but they are not considered as real neurons, cells differentiate into neuron-like cells. NGF effect on the PC12 cell line is reversible.

The PC12 cell line is a widely used model in *in vitro* studies of neuronal differentiation and neurosecretion [47].

2.7.3 NTERA-2

The NTERA-2 cell line is a pluripotent human embryonal carcinoma cell line. The NTERA-2 cells share many developmental and biochemical characteristics similar to the early-embryonal cells.

NTERA-2 cells are able to differentiate into glial cells and neurons. The differentiation of NTERA-2 cell line to neurons is mediated through receptors for retinoic acid.

NTERA-2 cells are important *in vitro* model for studying terminal differentiation and human neurogenesis [48].

2.8 *In vivo* rodent models

2.8.1 Models of AD

2.8.1.1 APP/PS1 mice

APP/PS1 mice are double transgenic mice. This mouse model combines human transgenes for APP with mutation found in inherited AD in a Swedish family and mutation in human presenilin-1 (PS1) gene. The human APP transgene is expressed three times more than murine APP. Transgenes are responsible for the formation of Aβ. Mice develop Aβ deposits in the cortex and hippocampus by the age of nine months. Impairment in spatial memory compared to their littermates tested in behavioral experiments is also observed in APP/PS1 mice [49].

2.8.1.2 THY-Tau22 mice

The transgenic THY-Tau22 mouse model is characterized by overexpression of 4-repeat human tau carrying two mutations, G272V and P301S, and parallel development of aggregation of hyperphosphorylated Tau protein in amygdala, hippocampus and other limbic brain structures. *Cornu ammonis* 1 (CA1) region of hippocampus is the first part of the brain affected by AD-like tauopathy [13,50,51].

At age of 6 months, NTF-like formations are developed in the CA1 region in hippocampi of THY-Tau22 mice. Hippocampus of 12 months old THY-Tau22 mouse shows aggregations of hyperphosphorylated Tau protein. Up to 16 months of age, NFT are observed in the cortex.

Cognitive function changes are also observed. Memory, spatial orientation and learning abilities are impaired. Possible damage can be observed in several behavioral tests such as Y-maze, Morris water maze or Barnes maze [50,52].

2.8.2 In vivo models of T2DM

2.8.2.1 db/db mice

Diabetic mice (db/db) are genetic model of T2DM. Due to mutation in diabetic gene (db) of leptin receptor, these mice have impaired leptin signaling which leads to increased levels of leptin. Consequently, db/db mice develop obesity, early-onset hyperinsulinemia and hyperglycemia.

The cortex and hippocampus of db/db mice have been shown to be associated

with increased Tau phosphorylation. These results of increased tau phosphorylation could be a key factor in the increased appearence of AD in diabetics [53].

2.8.2.2 MSG mice

MSG mouse model is characterized by monosodium glutamate-induced obesity, hyperleptinemia and hyperinsulinemia. New born mice are subcutaneously administered with monosodium glutamate (MSG) the second to the fifth day after birth. This causes a lesions in the *arcuate nucleus* (ARC) in the hypothalamus. ARC is important centre for food intake regulation. These specific lesions in the ARC causes imbalance between food intake and energy expenditure [54].

Due to MSG-induced obesity, MSG mice develop insulin resistance. Špolcová et al. (from Dr. Maletínská group IOCB AS CR) demostrated that MSG mice at the age of 6 months developed central insulin resistance with subsequent hyperphosphorylation of Tau protein at epitopes Ser396 and Thr231 in the hippocampi compared to their controls. MSG mice were treated for 2 weeks with a lipidized analogue of PrRP and liraglutide. Both peptides have a central anorexigenic effect. A two-week-long subcutaneous treatment resulted in increased phosphorylation of kinases PDK1 (Ser 241), Akt (Thr308) and GSK-3β (Ser9) in insulin signaling pathway. Furthermore, lower phosphorylation at Thr231, Thr212 and Ser396 of Tau protein was observed after the treatment [21].

2.8.2.3 Zucker fatty (fa/fa) rats

Zucker fatty (fa/fa) rat is a spontaneous genetic model of pre-diabetes, obesity and hypertension. Zucker fatty rats carry leptin receptor mutation which leads to rapid accumulation of adipose tissue and early-onset obesity. Leptin dysfunction is responsible for increased food intake and decreased energy expenditure. fa/fa rats are resistant to leptin and insulin and exhibit hyperleptinemia and hyperinsulinemia [55].

In study on fa/fa rats from Špolcová et al. (from Dr. Maletínská group IOCB AS CR) was determined that obesity and aging are risk factors for central insulin resistance which is related to the pathological hyperphosphorylation of Tau protein. It was observed that obesity and aging significantly decreased activation of insulin signaling pathway kinases (Akt, GSK-3β) in hippocampi of fa/fa rats. Furthermore, it was

concluded that the hyperphosphorylation of Tau protein at epitopes Ser396 and Thr231 in hippocampi of fa/fa rats was significantly increased by obesity and aging [27].

2.8.2.4 Koletsky rats

The Koletsky rat (SHROB, spontaneously hypertensive obese rat) is a unique strain characterized by obesity, hypertriglyceridemia, hyperinsulinemia/insulin resistance and develops renal disease. The strain has genetically determined hypertension as a offspring of female spontaneously hypertensive rat (SHR) and normotensive male. Koletsky rats carry a nonsense leptin receptor mutation [56,57]

According to previous studies on MSG mice [21] and fa/fa rats [27], Koletsky rats as a model of metabolic syndrome were chosen to study possible impairment in insulin signaling pathway leading to pathological hyperphoshorylation of Tau protein. Obesity and other parts of metabolic syndrom were proven as a risk factors for central insulin resistance with subsequent pathological hyperphosphorylation of Tau protein in previous studies described more in detail in chapters 2.8.2.2 and 2.8.2.3.

2.9 Behavioral tests

2.9.1 Y-maze

Y-maze is used for spatial short-term memory testing. Y-maze is a simple test consisting of three symmetrically mounted identical arms, as shown in Fig. 5. The test is based on the natural characteristics of rodents tendency to explore novel enviroments. Rodents use their visual recognition and spatial short-term memory which is hippocampus-dependent [58].

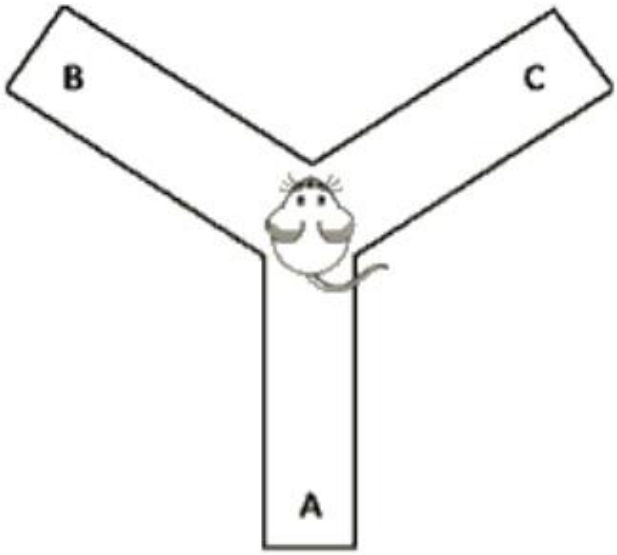

Fig. 5 Y-maze [59]

2.9.2 Morris Water Maze

Morris Water Maze (MWM) is a navigation task used for learning and spatial memory testing in rodents, widely used in neurosciences. MWM consists of large circular water tank with hidden platform placed about 0,5 cm below water surface. [60]

2.9.3 Barnes maze

Barnes maze (BM) was developed by Dr. Carol Barnes. BM is a tool used for spatial memory and learning testing.

BM consists of a circular open platform with 18-20 holes around its circumference. Under one of the holes, target escape hole is located. This task is frequently used in neurosciences to identify cognitive deficits and neurodegeneration in trangenic rodents [61].

2.9.4 Open Field Maze

Open Field Maze (OFM) is one of the most widely used behavioral test. OFM is used as an easy task to define behavior with no training of the subject. Rodents have natural aversion to brightly lit places, nevertheless they naturally tend to explore new enviroments. OFM is a behavioral anxiety-based test.

OFM is an arena marked with grid with walls around. The centre of OFM is colored to differentiate from other squares of the field [62].

3 MATERIALS & METHODS

3.1 Materials

3.1.1 Chemicals

Table 1 Summary of chemicals

Chemicals	Manufacturer
3-(4,5-Dimethylthiazol-2-yl)-2,5-Diphenyltetrazolium Bromide (MTT)	Sigma, St. Louis, MO, USA
Acrylamide	Sigma, St. Louis, MO, USA
Ammonium Persulfate (APS)	Sigma, St. Louis, MO, USA
Bovine Serum Albumin (BSA)	Serva GmbH, Heidelberg, Germany
Complete Protease Inhibitor Cocktail	Roche Diagnostics GmbH, Mannheim, Germany
Luminata Classico/Crescendo/Forte	Merck Millipore Headquatres, Billerica, MA, USA
Methanol	PENTA, Chrudim, Czech Republic
NaCl	Sigma, St. Louis, MO, USA
NaF	PENTA, Chrudim, Czech Republic
Na_3VO_4	Sigma, St. Louis, MO, USA
N,N,N′,N′- Tetramethylethyldiamin (TEMED)	Sigma, St. Louis, MO, USA
N,*N*′-Methylenebisacrylamide (Bisacrylamide)	Sigma, St. Louis, MO, USA
Precision Plus Protein™ Dual Color/All Blue Standard	BioRad, Hercules, CA, USA
Sodium Dodecyl Sulfate (SDS)	Sigma, St. Louis, MO, USA
Sodium Deoxycholate	Sigma, St. Louis, MO, USA
Trizma Base (Tris)	Sigma, St. Louis, MO, USA
Tween-20	Serva GmbH, Heidelberg, Germany
XT MOPS Running Buffer	BioRad, Hercules, CA, USA
β-Mercaptoethanol	Sigma, St. Louis, MO, USA

Other commonly used chemicals were purchased in p.a. quality from Sigma Aldrich (St. Louis, MO, USA).

3.1.3 Instruments

BioSafety Cabinet EuroFlow EF/S4, Clean Air, Woerden, Netherlands

Bullet Blender homogenizer, Next Advanced, Inc., Averill Park, NY, USA

ChemiDoc™, Bio-Rad, Herkules, CA, USA

Centrifuge HETTICH Univerzal 320, Tuttlingen, Germany

Centrifuge MiniSpin, Eppendorf AG, Hamburg, Germany

CO2 incubator MCO 18AIC, Sanyo, Osaka, Japan

CRITERION ™ Cell, BioRad, Hercules, CA, USA

CRITERION ™ Blotter, BioRad, Hercules, CA, USA

ELISA reader Infinite F50, TECAN Group Ltd., Männedorf, Switzerland

Mini-Protean 3, BioRad, Herkules, CA, USA

StandAxiovert 40 CFL microscope, Zeiss, Oberkochen, Germany

ThermoShaker PST-60HL-4, BIOSAN, Riga, Latvia

XCell SureLock, Invitrogen, NY, USA

3.1.4 Material

Cell Culture Dishes, Nunc, Roskilde, Denmark

CRITERION™ XT Precast Gel, 4-12 % BisTris, 1 mm, BioRad, Hercules, CA, USA

CytoTox 96® Non-Radioactive Cytotoxicity Assay, Promega Corporation, Madison, WI, USA

Pierce ™ BCA Protein Assay Kit, ThermoFisher Scientific, Inc., Waltham, MA, USA

3.2 Peptides

3.2.1 Human PrRP31 and palm^{11}-PrRP31

Human PrRP31 with the structure: SRTHRHSMEIRTPDINPAWYASRGIRPVGRF-NH2 and palmitoylated analog of PrRP31, palm^{11}-PrRP31, with the structure: SRTHRHSMEI K γ-E (N-palmitoyl) TPDINPAWYASRGIRPVGRF-NH2, were synthesized and purified at the Institute of Organic Chemistry and Biochemistry, Academy of Science of the Czech Republic (IOCB AS CR), Prague, Czech Republic as previously described [44].

The identity and purity of the peptides was determined using HPLC and Q-TOF micro MS technique (Waters, Milford, MA, USA).

3.2.2 Liraglutide

Liraglutide was purchased from NovoNordisk, Bagsvaerd, Denmark as Victoza®, prefilled multi-dose pen.

3.3 *In vitro* experiments

SH-SY5Y cell line was cultured in DMEM (Dulbecco's modified eagles medium) growth medium with a heat-inactivated fetal bovine serum (FBS) in final concentration of 10 %, 2 mmol·dm^{-3} L-glutamin, 1 % non-essential amino acids and penicilin/streptomycin in final concentration of 1 %. Cell line was maintained at 37 °C in 95 % air/5 % CO_2 humidified atmosphere. Medium was changed every 4-5 days. SH-SY5Y cells grow as adherent cells.

SH-SY5Y cells were cultured at density of $4 \cdot 10^{4}$ cells per well in 96-well plates. 16-18 hours before experiment, growth media was carefully aspirated from the cell culture and DMEM serum-free media (2 mmol·dm^{-3} L-glutamin, 1 % penicilin/streptomycin, 1 % non-essential amino acids) was added into each well. After 16-18 hours, peptides (at final concentrations $1 \cdot 10^{-5}$ mol·dm^{-3}or $1 \cdot 10^{-7}$ mol·dm^{-3}were added to media as a pretreatment and after 4 hours of incubation at 37 °C with peptides methyglyoxal (MG) was added to media at final concentration 1,2 mmol·dm^{-3}. Cell were incubated with MG for 24 hours. Next day, MTT test was chosen to measure cell viability and lactate dehydrogenase (LDH) test to measure methyglyoxal-induced cytotoxicity. Both tests were performed following manufacturer's protocol.

3.3.1 Methylglyoxal

Methylglyoxal (MG) is highly reactive product of several metabolic pathways such as lipid peroxidation, oxidative degradation of glucose or glycolysis. Accumulation of MG can negatively affect proteins and nucleic acids which leads to cellular dysfunction and inhibited proliferation.

Increased levels of plasma MG are found in AD brains, same as increased levels of pro-apoptotic Bax protein and caspase-3 which is critical in apoptosis onset, and decreased levels of anti-apoptic Bcl2. All these findings lead to one of the early apoptotic events, decreased mitochondrial transmembrane potential [63]. MG was chosen as a stressor which compromises energy metabolism of SH-SY5Y cells to

simulate metabolism in neurons affected by AD.

3.3.2 MTT assay

MTT assay is tetrazolium-based assay used for detection of viable cells. Active mitochondrial dehydrogenasis of living cells can reduce tetrazolium reagent depending on ability of nicotinamide adenine dinucleotide phosphate (NAPDH) – dependent cellular oxidoreductases to water insoluble purple formazan.

After 24-hour-long incubation with MG, MTT solution was added to each well and plate was incubated for 3-4 hours at 37 °C. After incubation, media was carefully aspirated. Dimethyl sulfoxide (DMSO) was added to each well to dissolve formazan. Absorbance was measured using ELISA reader at wavelength of 560 nm.

3.3.3 LDH assay

LDH assay is a colorimetric method to measure lactate dehydrogenase (LDH) as a biomarker of membrane disintengrity for cellular cytotoxicity and cytolysis. Cytotoxicity is measured as a level of extracellular LDH, released upon cell lysis. Activity of extracellular LDH relies on general chemical reaction (Fig. 6) and is measured with coupled enzymatic assay which converts iodonitrotetrazolium violet (INT) into red color formazan product.

After incubation with MG, the CytoTox 96® Non-Radioactive Cytotoxicity Assay was used following the assay protocol. 100 % DMSO was used for its well known cytotoxic properties as a comparator for the MG-cytotoxic effects.

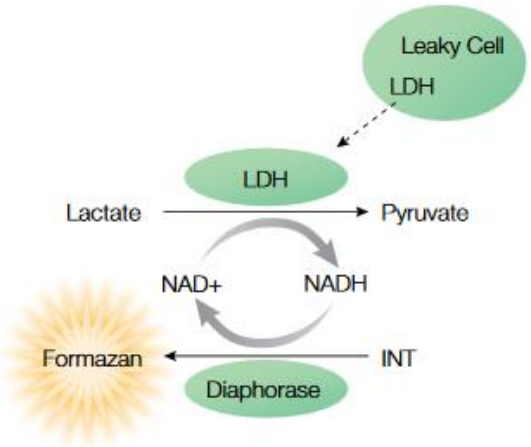

Fig. 6 General chemical reaction of LDH assay [64]

3.4 *In vivo* experiments

In vivo experiments were performed in the Czech Republic and followed the ethical guidelines for animal experiments and the Czech Republic Act No. 246/1992. All *in vivo* experiments were approved by the Committee fo Experiments with Laboratory Animals of Academy of Sciences of the Czech Republic

.

3.4.1 THY-Tau22 mice

5-month-old THY-Tau22 female mice and their age- and sex-matched wild-type (WT) controls were obtained from INSERM Laboratory UMR-S-1172, Alzheimer & Tauopathies , Lille, France and were housed with 12-12 hour light-dark cycle and constant temperature 23 ± 2 °C in Animal facility of the Institute of Physiology AS CR, Prague, Czech Republic with water and Altromin diet (Altromin, Eastern Westphalia, Germany) *ad libitum*.

THY-Tau22 female mice were housed 3-4 mice per cage. From the age of 7 months, mice were infused with palm^{11}-PrRP31 dissolved in phosphate-buffered saline (PBS)/5 % Tween 80 pH = 6 (dose 5 mg·kg^{-1} of body weight per day) using subcutaneous Alzet® osmotic pumps (Alzet, Cupertino, CA, USA) for 2 months. THY-Tau22 control mice and WT control mice were infused with PBS/ 5 % Tween 80. Alzet® osmotic pumps were implanted and changed after one month of the treatment in short-term anesthesia. Body weight and food intake of THY-Tau22 mice was measured three times per week.

For hippocampal-dependent spatial short-term memory testing Y-maze task was chosen. Y-maze task was performed before starting the treatment and after 2 months of treatment with palm^{11}-PrRP31. Y-maze is composed of 3 symmetrical arms. A mouse was first placed at the end of a start arm and allowed to explore 2 of 3 arms for 5 min. After 5 min, the mouse rested outside the maze for 2 min and then was placed into the maze with all 3 arms opened for 1 min. The time spent in novel arm was measured. The Y-maze and software for time measurement were created in the Development Centre of IOCB AS CR, Prague.

At the end of the experiment, overnight fasted THY-Tau22 mice and their WT controls were sacrificed by decapitation. Blood glucose concentrations were measured by glucometer Glucocard (Arkray, Tokyo, Japan). Concentration of plasma leptin was

measured by ELISA kit (Millipore, USA) and insulin level was determined by radioimmunoassay kits (Millipore, USA) following the manufacturer's protocol. The liver and the subcutaneous and visceral fat (WAT) were dissected, weight and frozen in liquid nitrogen and stored at -80 °C. The hippocampi were separated from the brains, frozen in liquid nitrogen and stored in cold lysis buffer, described more in detail in chapter 3.4.3. below.

3.4.2 Koletsky rats (SHROB)

6-week-old SHROB male rats and their age-and sex-matched SHR controls were purchased from Charles River (Wilmington, USA). Rats were housed with 12-12 hour light-dark cycle and constant temperature 22 ± 2 °C in Animal facility of the Institute of Physiology AS CR, Prague, Czech Republic with water and Ssniff diet (Spezialdiäten GmbH, Soest, Germany) *ad libitum*.

The SHROB male rats were IP administered with palm^{11}-PrRP31 (at a dose 5 mg·kg^{-1} of body weight) once-daily at 15:00 h for 3 weeks. SHROB male rats were housed 2 rats per cage.

BW and food intake of rats was measured every two days during the treatment. Overnight fasted Koletsky rats were sacrificed by decapitation. After decapitation, blood and tissue samples were collected. Blood was obtained from the tail vessel. Blood glucose concentrations were measured by using glucose oxidase method (8/28 Biosen S Line, EKF Diagnostics, Barleben, Germany). Concentration of plasma leptin and insulin levels were determined by using radioimmunoassay kits (Millipore, USA) following the manufacturer's protocol. The symmetrical half of the WAT was weighed The hippocampi were dissected, frozen in liquid nitrogen and stored in cold lysis buffer, described more in detail in chapter 3.4.3. below.

3.4.3 Hippocampi preparation for immunoblotting

After decapitation, hippocampi were isolated from the dissected brains, placed to cold lysis buffer (62,5 mmol·dm^{-3} Tris-HCl buffer with pH = 6,8, 1 % sodium dodecylcholate, 1 % Triton X-100, complete protease inhibitor (Roche Applied Science, Mannheim, Germany), 50 mmol·dm^{-3} NaF, 1 mmol·dm^{-3} Na_3VO_4) and stored at -20 °C. Aterwards, the samples were homogenized using a Bullet Blender homogenizer (Next

Advanced, Inc., Averill Park, NY, USA) and sonicated for 1 min. Using Pierce ™ BCA Protein Assay Kit (ThermoFisher Scientific, Inc., Waltham, MA, USA), protein concentration was measured according to manufacturer's instructions. The individual samples were diluted in a Laemmli sample buffer (62,5 $mmol \cdot dm^{-3}$ Tris-HCl pH = 6,8 with the addition of 2 % SDS, 10 % glycerol, 1 % bromophenol blue, 0.5 % β-mercaptoethanol, 50 $mmol \cdot dm^{-3}$ NaF, 1 $mmol \cdot dm^{-3}$ Na_3VO_4) to a final concentration $1 \mu g \cdot \mu l^{-1}$ and stored at -20 °C.

3.4.4 Immunoblotting

3.4.4.1 Gel Electrophoresis

The samples for immunoblotting were sonicated for 1 minute, boiled at 100 °C for 2 minutes and centrifuged for 5 minutes . Then, 10 µl of each sample was subjected to 4-12 % Bis Tris CRITERION™ XT Precast Gel with CRITERION™ Cell electrophoresis with XT MOPS as a running buffer (Bio-Rad, Hercules, CA, USA) at constant voltage 200 V for 40 minutes.

3.4.4.2 Protein transfer onto nitrocellulose membrane

The proteins were transferred onto a nitrocellulose membrane using CRITERION™ Blotter (Bio-Rad, Hercules, CA, USA) with blotting buffer (25 $mmol \cdot dm^{-3}$ Tris, 192 $mmol \cdot dm^{-3}$ glycin, 20 % methanol) at constant voltage 100 V for 45 minutes

.

3.4.4.3 Immunodetection of phosphorylated and non-phosphorylated proteins

The blots were blocked in 5 % non-fat milk or BSA in TBS/Tween-20 buffer (20 $nmol \cdot dm^{-3}$ Tris, 136 $mmol \cdot dm^{-3}$ NaCl, 0.1 % Tween-20, 50 $mmol \cdot dm^{-3}$ NaF, and 5 $mmol \cdot dm^{-3}$ Na_3VO_4) and overnight incubated in the primary antibody with appropriate dilution shown in Tab. 2 at 4 °C. Then membranes were incubated for 1 hour with the HRP-linked secondary antibody (Tab. 3) at room temperature, the membranes were developed using Luminata Classico/Crescendo/Forte Western HRP Substrates. The bands were visualized in a ChemiDoc™ System and quantified using Image Lab Software (Bio-Rad, Hercules, CA, USA). The intensity of the bands with the phosphorylated protein and the intensity of the band with the total level of the protein

were calculated.

Table 2 Summary of primary antibodies and their dilution

Antibody	Dilution	Manufacturer
Rabbit polyclonal antibody AD2 (pTau protein Ser396, 404)	1:5 000 5 % BSA TBS/Tween20	Produced in INSERM Laboratory UMR-S-1172, Lille, France
Rabbit monoclonal antibody against Phospho-Akt (Ser473)	1:1 000 5 % BSA TBS/Tween20	Cell Signaling Technology, Beverly, MA, USA
Rabbit monoclonal antibody against Phospho-Akt (Thr308)	1:1 000 5 % BSA TBS/Tween20	Cell Signaling Technology, Beverly, MA, USA
Mouse monoclonal antibody AT8 (pTau protein Ser202, Thr205)	1:1 000 5 % BSA TBS/Tween20	ThermoFisher Scientific, Inc., Waltham, MA, USA
Mouse monoclonal antibody AT180 (pTau protein Thr231)	1:1 000 5 % BSA TBS/Tween20	ThermoFisher Scientific, Inc., Waltham, MA, USA
Mouse monoclonal antibody against BDNF (brain-derived neurotrophic factor)	1:2 000 5 % BSA TBS/Tween20	abcam, Cambridge, UK
Rabbit monoclonal antibody against cdk5	1:2 000 5 % BSA TBS/Tween20	Cell Signaling Technology, Beverly, MA, USA
Rabbit monoclonal antibody against doublecortin	1:1 000 5 % non-fat milk TBS/Tween20	Cell Signaling Technology, Beverly, MA, USA
Mouse monoclonal antibody against phospho-GSK-3β (Ser9)	1:1 000 5 % BSA TBS/Tween20	Cell Signaling Technology, Beverly, MA, USA

Rabbit monoclonal antibody against total GSK-3β	1:1 000 5 % BSA TBS/Tween20	Cell Signaling Technology, Beverly, MA, USA
Rabbit monoclonal antibody against total PDK1	1:1 000 5 % BSA TBS/Tween20	Cell Signaling Technology, Beverly, MA, USA
Rabbit monoclonal antibody against phospho-PDK1 (Ser241)	1:1 000 5 % BSA TBS/Tween20	Cell Signaling Technology, Beverly, MA, USA
Rabbit monoclonal antibody against PI3 Kinase p85	1:1 000 5 % BSA TBS/Tween20	Cell Signaling Technology, Beverly, MA, USA
Rabbit monoclonal antibody against protein phosphatase PP2A subunit C	1:1000 5 % non-fat milk TBS/Tween20	Cell Signaling Technology, Beverly, MA, USA
Rabbit polyclonal antibody against PSD95	1:1 000 5 % BSA TBS/Tween20	Cell Signaling Technology, Beverly, MA, USA
Rabbit polyclonal antibody against Synaptophysin	1:1 000 5 % BSA TBS/Tween20	Santa Cruz Biotechnology, Dallas, TX, USA
Mouse monoclonal antibody Tau5 antibody	1:10 000 5 % non-fat milk TBS/Tween20	Invitrogen Corporation, Frederick, MD, USA
Mouse monoclonal antibody against α-GAPDH	1:10 000 5 % cassein TBS/Tween20	Gift from Konvalinka group, IOCB AS CR
Mouse monoclonal antibody against β-actin	1:10 000 5 % non-fat milk TBS/Tween20	Sigma, St. Louis, MO, USA

Table 3 Summary of secondary antibodies and their dilution

Antibody	Dilution	Manufacturer
Anti-mouse IgG HRP-linked antibody	1:2 000	Cell Signaling Technology, Beverly, MA, USA
Anti-rabbit IgG HRP-linked antibody	1:2 000	Cell Signaling Technology, Beverly, MA, USA

Secondary antibodies listed in Table 3 were diluted in TBS/Tween20 buffer.

3.4.4.4 α-GAPDH and β-actin detection

To compare the total level of the proteins in individual samples, α-GAPDH or β-actin were used as an internal loading control.

Membranes were incubated for 60 minutes with a α-GAPDH or β-actin antibody at room temperature. These antibodies were diluted in a blocking buffer (TBS/0,1 % Tween20, 5 % non-fat milk, 1 mmol·dm^{-3} Na_3VO_4, 50 mmol·dm^{-3} NaF). After 90 minutes, membranes were incubated for 60 minutes with a secondary anti-mouse IgG antibody. The bands were visualized in a ChemiDoc™ System and quantified using Image Lab Software (Bio-Rad, Hercules, CA, USA).

The intensities of protein bands described in previous chapter 3.4.4.3 were normalized to β-actin or α-GAPDH as a internal loading control, and the ratios of the intensity of the band with the phosphorylated protein and the intensity of the band with the total level of the protein were calculated.

3.5 Statistical analyses

Data are presented as mean ± standard error of the mean (SEM). Differences between mean values were determinated using Student's t-test or 1-way ANOVA with Dunnett's post-hoc test. Differences of $p < 0.05$ were considered statistically significant. The data were analyzed in GraphPad Prism Software (San Diego, CA, USA).

4 RESULTS

4.1 Effect of palm^{11}-PrRP31 on MG-induced cytotoxicity

SH-SY5Y cells were treated with PrRP31, palm^{11}-PrRP31 or liraglutide in the absence or presence of 1,2 mmol·dm^{-3}MG which is highly cytotoxic and causes apoptosis to examine whether MG or tested peptides negatively affect cell viability and to determine the potent neuroprotective effect of PrRP31, palmitoylated analog of PrRP31, palm^{11}-PrRP31, and liraglutide in MG-induced toxicity.

4.1.1 Effect of tested peptides and pretreatment with tested peptides on SH-SY5Y cell viability with MG-induced apoptosis

MTT test was performed to measure effect of peptides studied on cell viability. Compared to blank as a control of non-treated living cells, cells treated with 1,2 mmol·dm^{-3} MG showed significant decrease in the cell viability as shown in Fig. 7a. No significant effect in cell viability was observed in SH-SY5Y treated with peptides themselves at concentration 1·10 $^{-5}$ or 1·10 $^{-7}$ mol·dm^{-3} compared to blank (Fig. 7a).

Neuroprotective effect of pretreatment with peptides was studied after incubation with cytotoxic MG at concentration 1.2 mmol·dm^{-3} on SH-SY5Y cell line (Fig. 7b). A significant increase in cell viability of SH-SY5Y cells was observed in cells pretreated with PrRP31 at concentration 1·10 $^{-5}$ mol·dm^{-3} and palm^{11}-PrRP31 in concentration 1·10 $^{-5}$ mol·dm^{-3}. No significant changes were found in cells pretreated with PrRP31 1·10 $^{-7}$ mol·dm^{-3}, palm^{11}-PrRP31 in concentration 1·10 $^{-7}$ mol·dm^{-3} and in liraglutide in concentration 1·10 $^{-5}$ mol·dm^{-3}.

a/

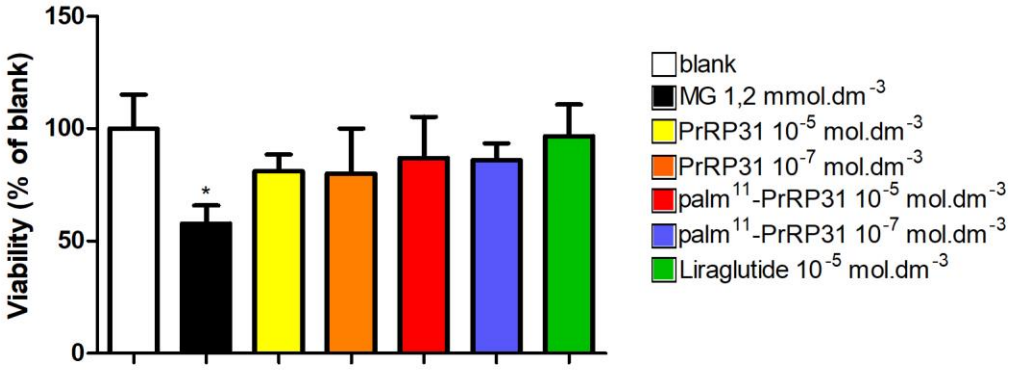

b/

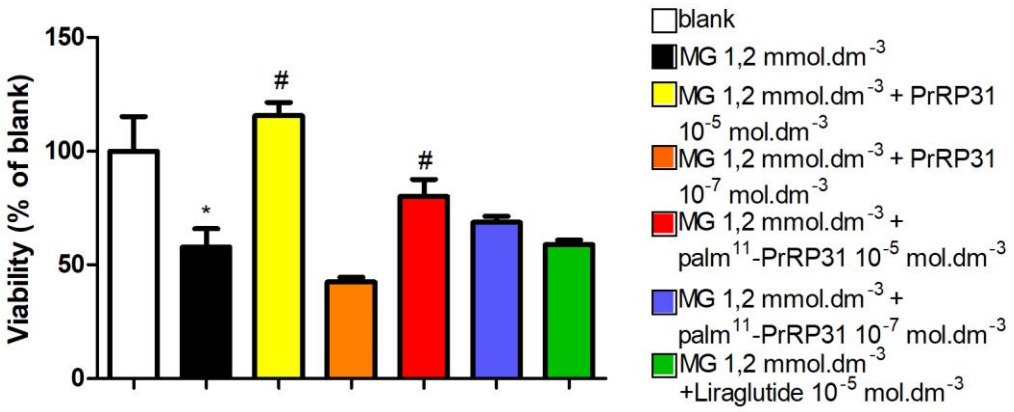

Fig. 7 Cell viability testing: a/ Effect of tested peptides on SH-SY5Y cell viability, b/Effect of pretreatment with tested peptides on SH-SY5Y cell viability with MG-induced apoptosis

*Data are mean ± SEM, n=3 repetition in quadruplicate. Statistical analysis was calculated by Student´s t-test. Significance is *P<0.05, #P<0.05. *MG vs blank, # treatment vs MG.*

4.1.2 Cytotoxic effect of MG and its attenuation by pretreatment of tested peptides on SH-SY5Y cells

To examine possible neuroprotective properties of tested peptides on MG-induce cytotoxic effect, LDH test as a analyze cell membrane disintegrity (Fig. 8) was performed on SH-SY5Y cell line. Cytotoxic effects of tested peptides were related to cytotoxic effect of DMSO which was determined as 100 %.

The 4-hour-long pretreatment of SH-SY5Y with PrRP31, palm^{11}-PrRP31 or liraglutide resulted in significantly decreased cytotoxicity which was induced by MG.

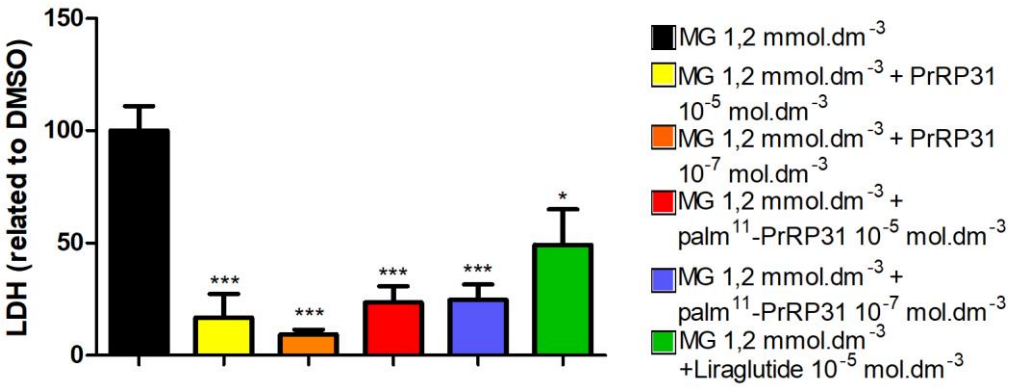

Fig. 8 Cytotoxicity testing: Neuroprotective effect of tested peptides against MG-induced cell death on SH-SY5Y cell line

*Data are mean ± SEM, n=3 repetition in quadruplicate. Statistical analysis was calculated by Student´s t-test. Significance is *P<0.05, ***P<0.001.*

4.2 Effect of the 2-month-long treatment with palm^{11}-PrRP31 in THY-Tau22 mice

The results from the experiments with THY-Tau22 mice were published by Popelová et al. [65], my part of this study involves participating in spatial memory testing, and performing and evaluating immunoblotting experiments.

4.2.1 Spatial memory testing

Y-maze task was used for spatial memory testing in THY-Tau22 mice before the beginning of the treatment and after 2-month-long palm^{11}-PrRP31 treatment.

Before the beginning of the experiment, the spatial memory in THY-Tau22 mice was impaired compared to WT control mice manifested by shorter time spent in the novel arm of the Y-maze (Fig. 9a).

Compared to PBS-treated THY-Tau22 mice, the spatial memory was improved in THY-Tau22 mice treated with palm^{11}-PrRP31 for 2 months, palm^{11}-PrRP31-treated THY-Tau22 spent significantly longer time in the novel arm of the Y-maze (Fig. 9b).

a/ Before intervention

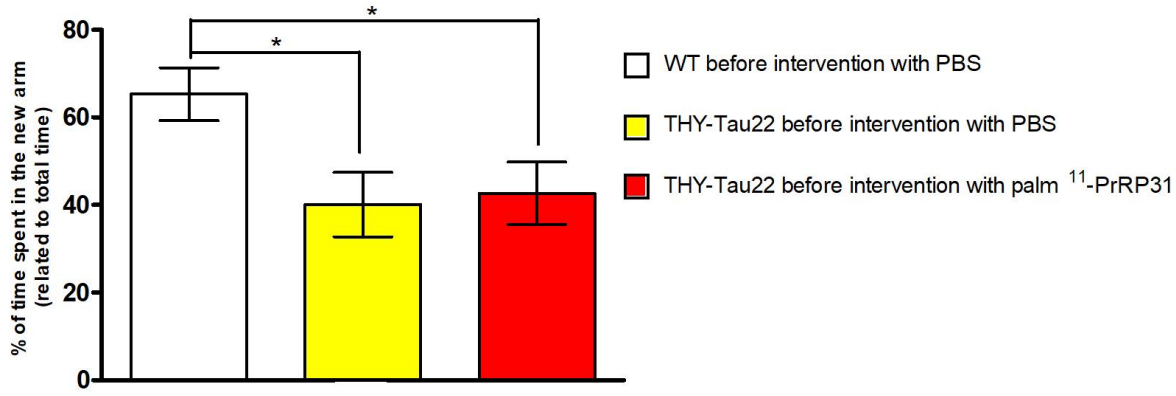

b/ After 2-month-long intervention

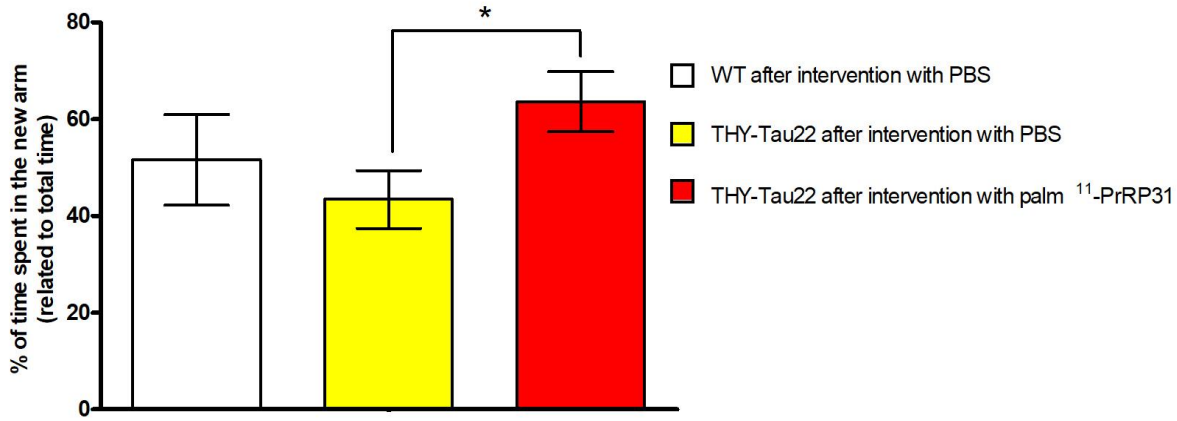

Fig. 9 Spatial memory testing of THY-Tau22 mice and their age- and sex-matched WT controls in the Y-maze task: a/ before intervention, b/ after 2-month-long intervention

*Data are mean ± SEM, n=6 mice per group. Statistical analysis was calculated by Student´s t-test. Significance is *P<0.05.*

4.2.2 Metabolic parameters

Cumulative food intake (Fig. 10) and the BW (Fig. 11) was measured during the 2-month-long palm^{11}-PrRP31 treatment. Compared to the THY-Tau22 control mice, the BW of WT control mice was significantly higher, despite of no significant changes in food intake among the groups. THY-Tau22 palm^{11}-PrRP31-treated mice did not displayed any significant changes in BW or food intake compared to THY-Tau22 controls.

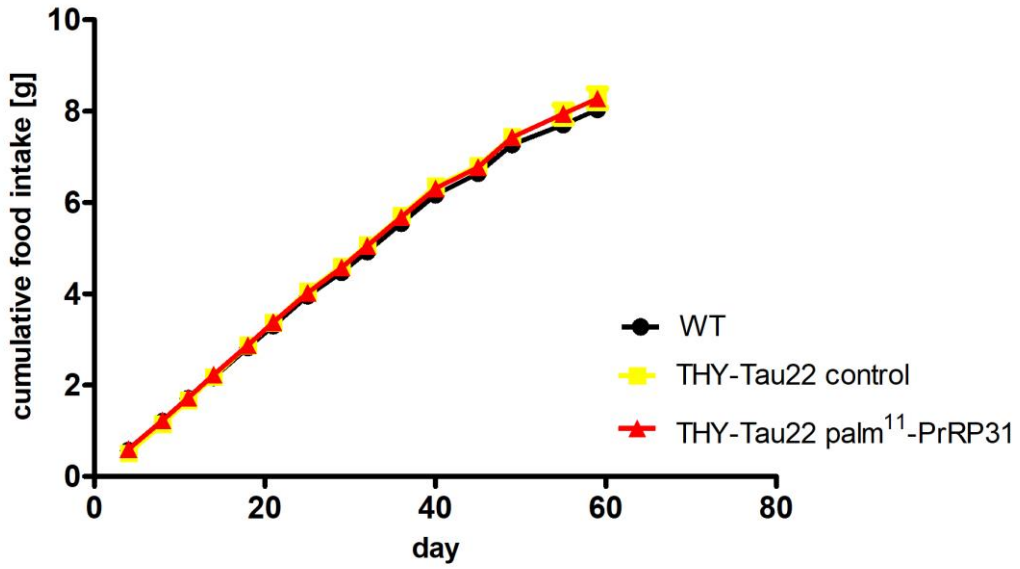

Fig. 10 Cumulative food intake during the 2-month-long treatment with palm^{11}-PrRP31

Cumulative food intake was measured 3 times per week during the palm^{11}-PrRP31 treatment (dose 5mg/kg/day) for 2 months. Data are mean ± SEM, n=6 mice per group. Statistical analysis was calculated by 1-way ANOVA.

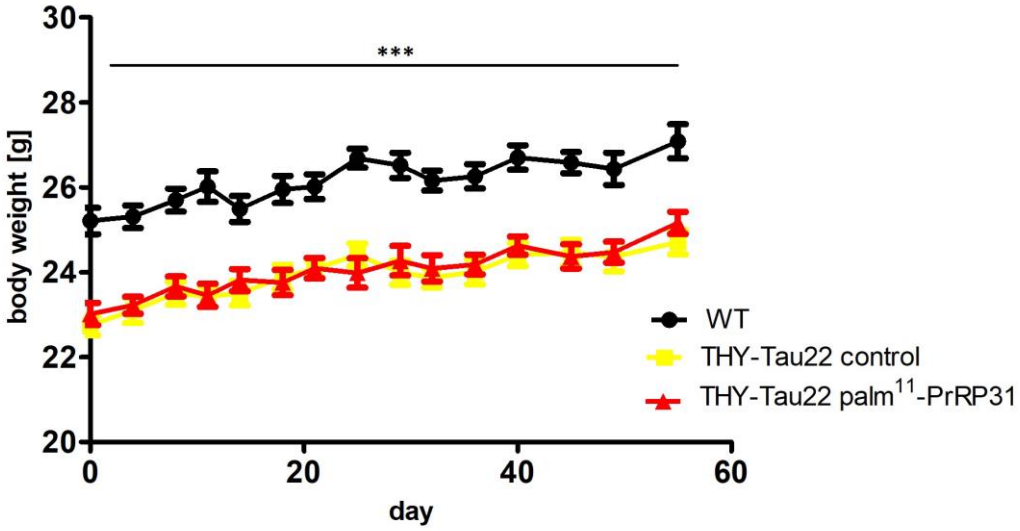

Fig. 11 Body weight change during the 2-month-long treatment with palm^{11}-PrRP31

*BW was measured 3 times per week during the palm^{11}-PrRP31 treatment (dose 5mg/kg/day) for 2 months. Data are mean ± SEM, n=6 mice per group. Statistical analysis was calculated by 1-way ANOVA with Dunnett post-hoc test. Significance is ***P<0.001. * THY-Tau22 PBS vs WT PBS.*

Metabolic parameters were measured after 2 months of palm^{11}-PrRP31 treatment (Table 4). There were no significant changes found in WAT weight and level of leptin, insulin or glucose.

Table 4 Metabolic parameters of THY-Tau22 mice and WT controls after the 2-month-long treatment

Genotype	BW [g]	WAT [% BW]	leptin [ng/ml]	insulin [ng/ml]	glucose [mmol/l]
WT controls	23,89±0,37***	2,16±0,11	0,51±0,12	0,19±0,04	4,59±0,30
THY-Tau22 controls	21,49±0,25	2,47±0,14	0,37±0,04	0,19±0,01	3,94±0,37
THY-Tau22 palm^{11}-PrRP31	21,82±0,28	2,77±0,23	0,52±0,07	0,21±0,02	4,72±0,33

*Data are mean ± SEM, n=6 mice per group. Statistical analysis was calculated by Student´s t-test. Significance is ***P<0.001. * THY-Tau22 PBS vs WT PBS.*

4.2.3 Effect of palm^{11}-PrRP31 treatment on hyperphosphorylation of human Tau protein and markers of neurogenesis

Immunoblotting analysis of hippocampi of THY-Tau22 mice treated with palm^{11}-PrRP31 and control mice for 2 months was performed.

Tau phosphorylation at Ser202 and Thr205 epitopes determined by AT8 antibody was non-significantly decreased and at Thr231 epitope determined by AT180 antibody was significantly decreased in THY-Tau22 treated with palm^{11}-PrRP31 compared to THY-Tau22 controls as shown in Fig. 12.

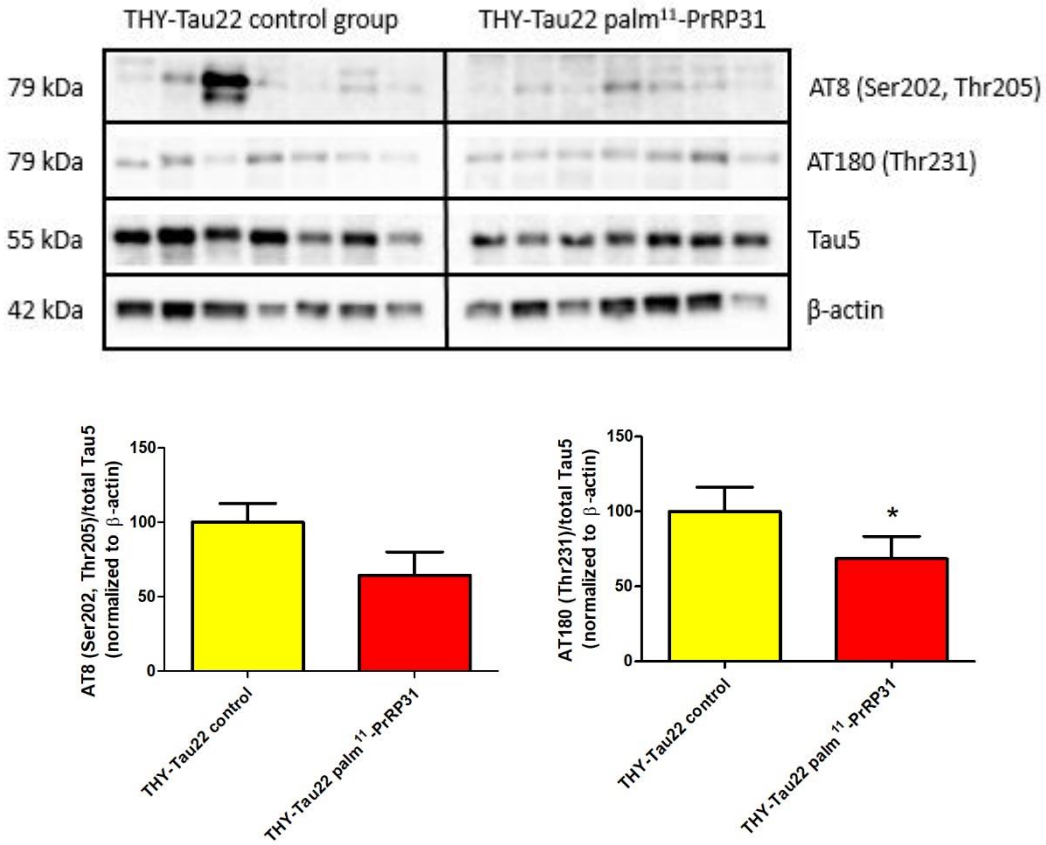

Fig. 12 Western blot analysis of human Tau protein phosphorylation at different epitopes in hippocampi of THY-Tau22 mice treated for 2 months with palm^{11}-PrRP31

*Data are mean ± SEM, n=6 mice per group. Statistical analysis was calculated by Student´s t-test. Significance is *P<0.05.*

As shown in Fig. 13, level of protein phosphatase 2 subunit C (PP2A sub C), which is able to dephosphorylate tau protein, was non-significantly increased in THY-

Tau22 palm^{11}-PrRP31-treated compared to THY-Tau22 controls.

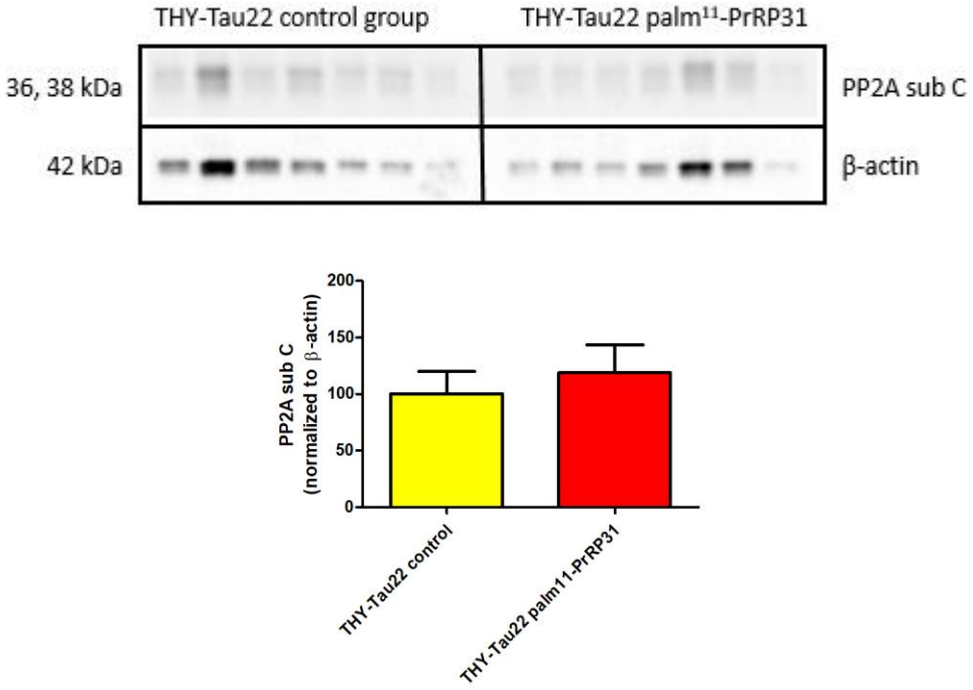

Fig. 13 Western blot of PP2A phosphatase implicated in Tau dephosphorylation in hippocampi of THY-Tau22 mice treated for 2 months with palm^{11}-PrRP31

Data are mean ± SEM, n=6 mice per group. Statistical analysis was calculated by Student´s t-test.

To examine the neuroprotective effect of palm^{11}-PrRP31 peptide, the brain-derived neurotrophic factor (BDNF) and doublecortin (Fig. 14) were also tested. The protein level of BDNF, a protein of neurotrophin family playing an important role in hippocampal synaptic plasticity, did not display different levels in palm^{11}-PrRP31-treated THY-Tau22 compared to PBS-treated THY-Tau22 controls.

There were no differences found in levels of doublecortin, which is a protein related to neurogenesis.

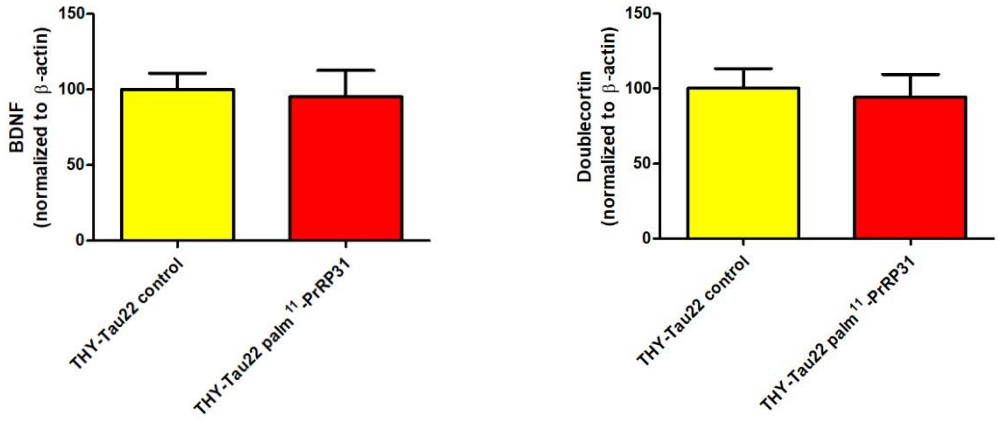

Fig. 14 Western blot analysis of markers of neurogenesis in hippocampi of THY-Tau22 mice treated for 2 months with palm^{11}-PrRP31

Data are mean ± SEM, n=6 mice per group. Statistical analysis was calculated by Student´s t-test.

4.3 Effect of the 3-week-long treatment with palm^{11}-PrRP31 in Koletsky rats (SHROB)

The results from the experiment with Koletsky rats were published by Mikulášková et al. [66], my part of this study involves performing immunoblotting.

4.3.1 Metabolic parameters

As shown in Fig. 15 and 16, the cumulative food intake and BW of Koletsky rats was measured every two days during the 3-week-long treatment with palm^{11}-PrRP31. Significant increase in food intake was found in SHROB control rats compared to SHR PBS-treated control group. No significant changes were found in BW or food intake in SHROB palm^{11}-PrRP31-treated rats compared to SHROB controls.

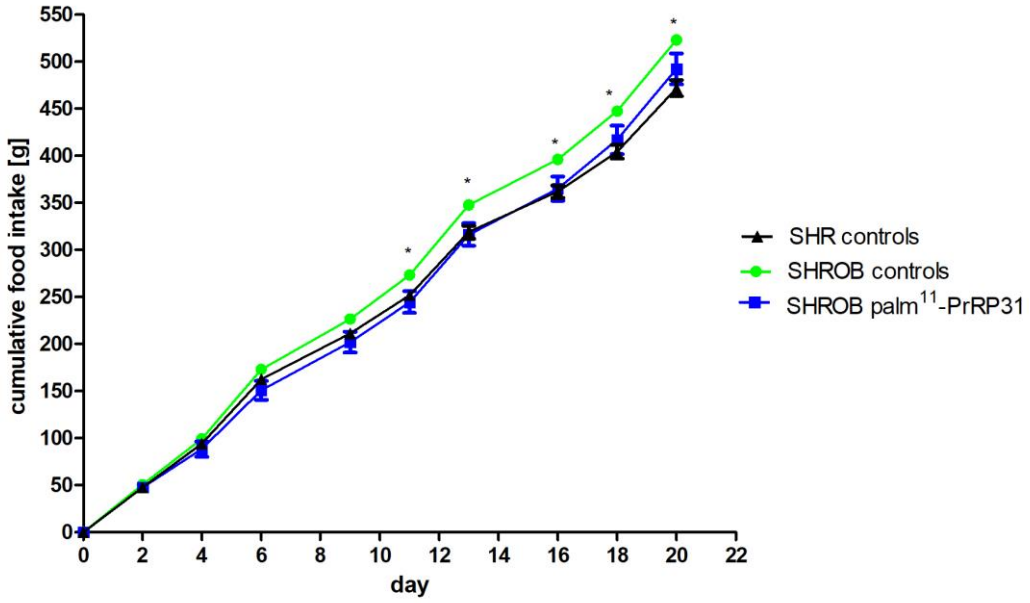

Fig. 15 Cumulative food intake during the 3-week-long treatment with palm^{11}-PrRP31

*Cumulative food intake was measured every 2 days during the palm^{11}-PrRP31 treatment (dose 5mg/kg/day) for 3 weeks. Data are mean ± SEM, n=8 rats per group. Statistical analysis was calculated by 1-way ANOVA with Dunnett post-hoc test. Significance is *P<0.05. *SHROB controls vs SHR controls.*

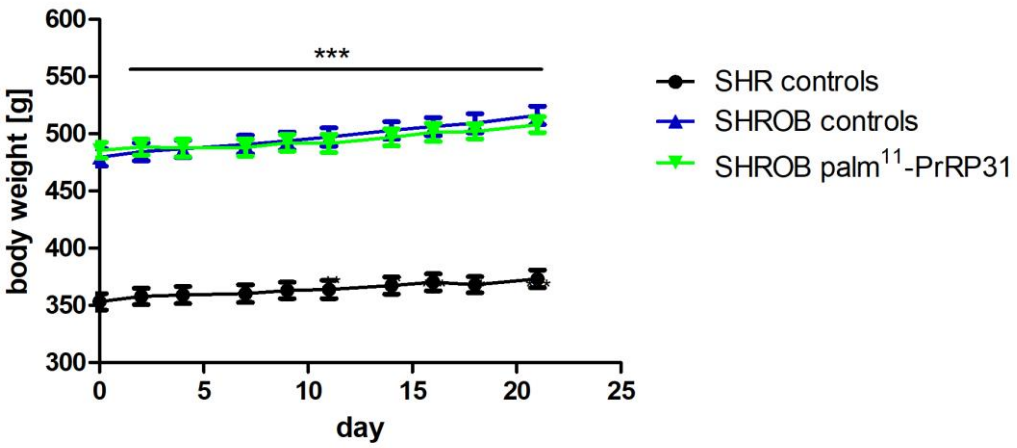

Fig. 16 Body weight change during the 3-week-long treatment with palm^{11}-PrRP31

*BW was measured 2 days during the palm^{11}-PrRP31 treatment (dose 5mg/kg/day) for 2 months. Data are mean ± SEM, n=8 rats per group. Statistical analysis was calculated by 1-way ANOVA with Dunnett post-hoc test. Significance is ***P<0.001. *SHROB controls vs SHR controls*

After the 3-week-long treatment with palm^{11}-PrRP31, metabolic parameters were measured.

Brains were dissected and weighed. Compared to SHR PBS-treated group, SHROB control group displayed significantly smaller brains. Non-significant changes were found in SHROB palm^{11}-PrRP31-treated rats compared to SHROB controls.

As shown in Tab. 5, compared to SHR control group, SHROB controls and SHROB palm^{11}-PrRP31-treated rats displayed significantly increased amount of the WAT. Level of leptin in blood plasma was significantly increased in SHROB controls and SHROB palm^{11}-PrRP31-treated rats compared to SHR control group. The insulin blood level was significantly higher in SHROB control group compared to SHR control rats. Compared to SHROB controls, significantly lower level of insulin in the blood was observed in SHROB palm^{11}-PrRP31-treated rats.

Table 5 Metabolic parameters of Koletsky rats after the 3-week-long palm^{11}-PrRP31 treatment

Genotype	BW [g]	brain weight [g]	½ WAT [% BW]	leptin [ng/ml]	insulin [ng/ml]	glucose [mmol/l]
SHR controls	373,00±8,00	1,90±0,06	1,89±1,70	3,97±1,30	0,72±0,23	3,88±0,20
SHROB controls	516,00±8,00***	1,67±0,07***	6,27±0,50***	179,13±24,84***	19,73±6,11***	4,44±0,59
SHROB palm^{11}-PrRP31	508,00±8,00	1,68±0,06	6,61±0,82	166,23±50,23	13,08±4,82#	4,02±0,20

*Data are mean ± SEM, n=8 rats per group. Statistical analysis was calculated by Student´s t-test. Significance is ***P<0.001, #P<0.05. * SHROB controls vs SHR controls, # SHROB palm^{11}-PrRP31 vs SHROB controls.*

4.3.2 Activation of Tau kinases, hyperphosphorylation of Tau protein and markers of neurogenesis and synaptogenesis

The effect of the 3-week-long treatment of palm^{11}-PrRP31 was examined using the method of immunoblot with specific antibodies in hippocampi of Koletsky rats and their SHR controls.

In the insulin signaling pathway shown in Fig. 17, the protein level of PI3K did not differ significantly between SHROB control rats and their SHR controls. In SHROB rats treated with palm^{11}-PrRP31, non-significant increased level of PI3K was observed compared to control group of SHROB rats.

The level of phosphorylation at epitope Ser241 of PDK1 did not display any significant changes in SHROB PBS-treated rats compared to SHR rats, neither in SHROB palm^{11}-PrRP31-treated compared to SHROB control rats.

The phosphorylation at Ser473 and Thr308 of kinase Akt did not show any significant changes. The phosphorylation at Ser473 epitope showed non-significant decrease in a group of control SHROB rats compared to SHR control group, same as SHROB palm^{11}-PrRP31-treated. On the other hand, the Akt phosphorylation at Thr308 was non-significantly increased in SHROB rats treated with palm^{11}-PrRP31 compared to SHROB control group. No significant changes were found in phosphorylation at Thr308 epitope of Akt in SHROB control group compared to SHR control rats.

Non-significant changes were also found in phosphorylation at inhibition epitope Ser9 of GSK-3β, the main Tau protein kinase.

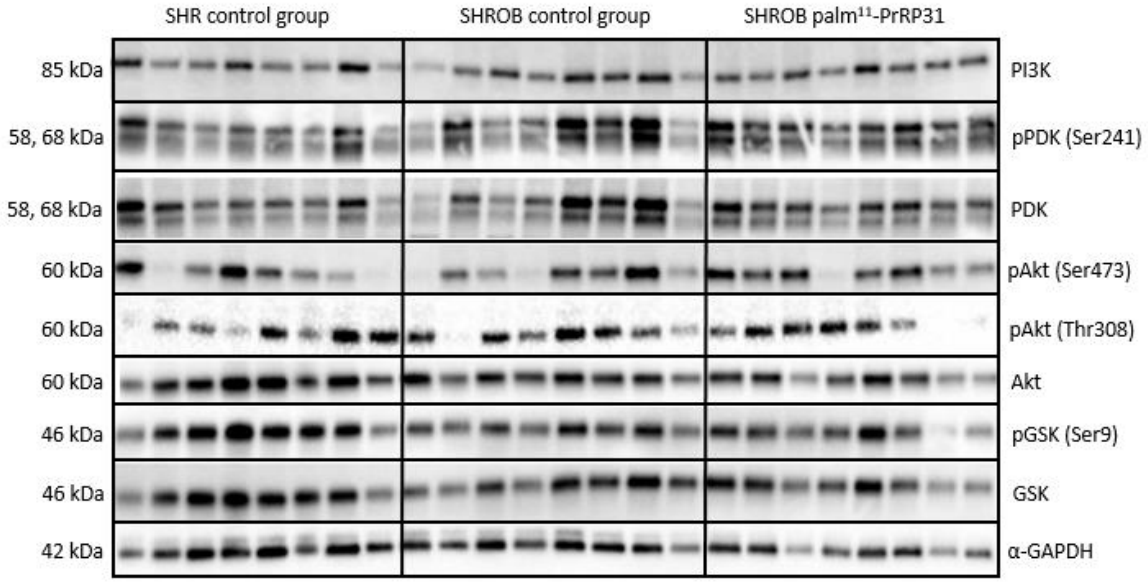

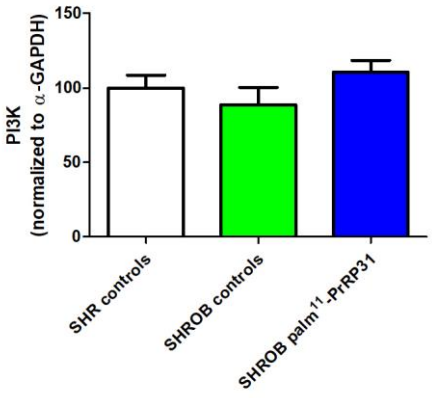

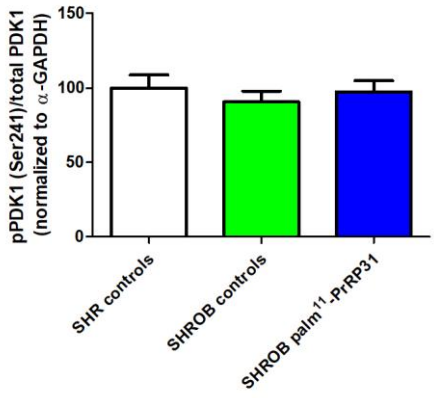

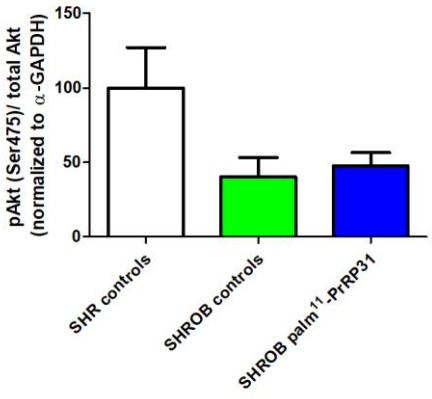

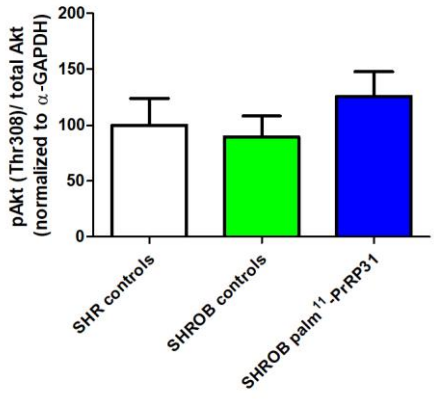

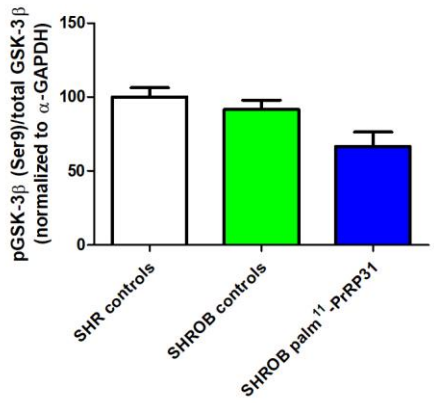

Fig. 17 Western blot analysis of kinases implicated in insulin signaling pathway in hippocampi of Koletsky rats treated for 3 weeks with palm^{11}-PrRP31

Data are mean ± SEM, n=8 rats per group. Statistical analysis was calculated by Student´s t-test.

As shown in Fig. 18, activity of kinases and phosphatase of Tau protein were measured.

A significant decrease of the phosphorylation of cdk5 was observed in SHROB group treated with palm^{11}-PrRP31compared to SHROB control rats. No significant changes were found in a group of control SHROB rats compared to SHR control group.

The phosphorylation of MAPK/Erk 1/2 at Thr202 and Tyr204 epitopes showed non-significant increase in SHROB group treated with palm^{11}-PrRP31compared to SHROB control group.

There were no significant changes found in levels of PP2A sub C.

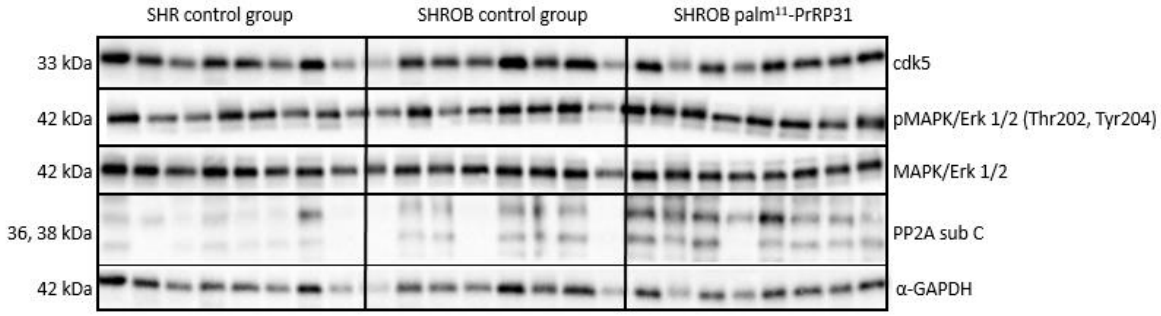

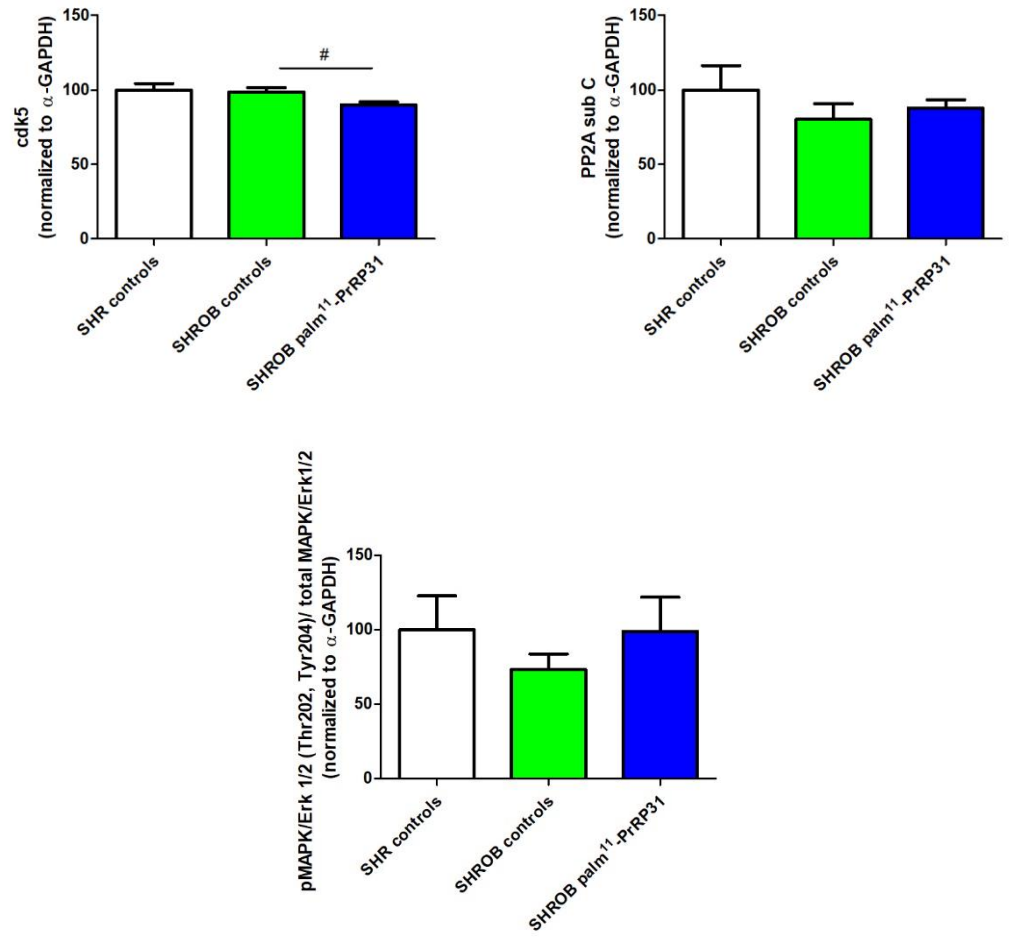

Fig. 18 Western blot analysis of kinases and phosphatase related to Tau protein in hippocampi of Koletsky rats treated for 3 weeks with palm^{11}-PrRP31

Data are mean ± SEM, n=8 rats per group. Statistical analysis was calculated by Student´s t-test. Significance is #P<0.05. # SHROB palm^{11}-PrRP31 vs SHROB controls.

The phosphorylation of Tau protein was measured (Fig. 19). At the epitopes Ser396 and Ser404 using AD2 antibody, phosphorylation of Tau protein was significantly increased in SHROB control group compared to control SHR rats. Compared with SHROB control rats, SHROB palm^{11}-PrRP rats displayed significantly decreased phosphorylation of Tau protein determined by AD2 antibody.

The phosphorylation of Thr231 was significantly increased in SHROB control group compared to their SHR controls. Lower phosphorylation, but non-significant, of Thr231 was observed in SHROB palm^{11}-PrRP-treated rats compared to SHROB control rats.

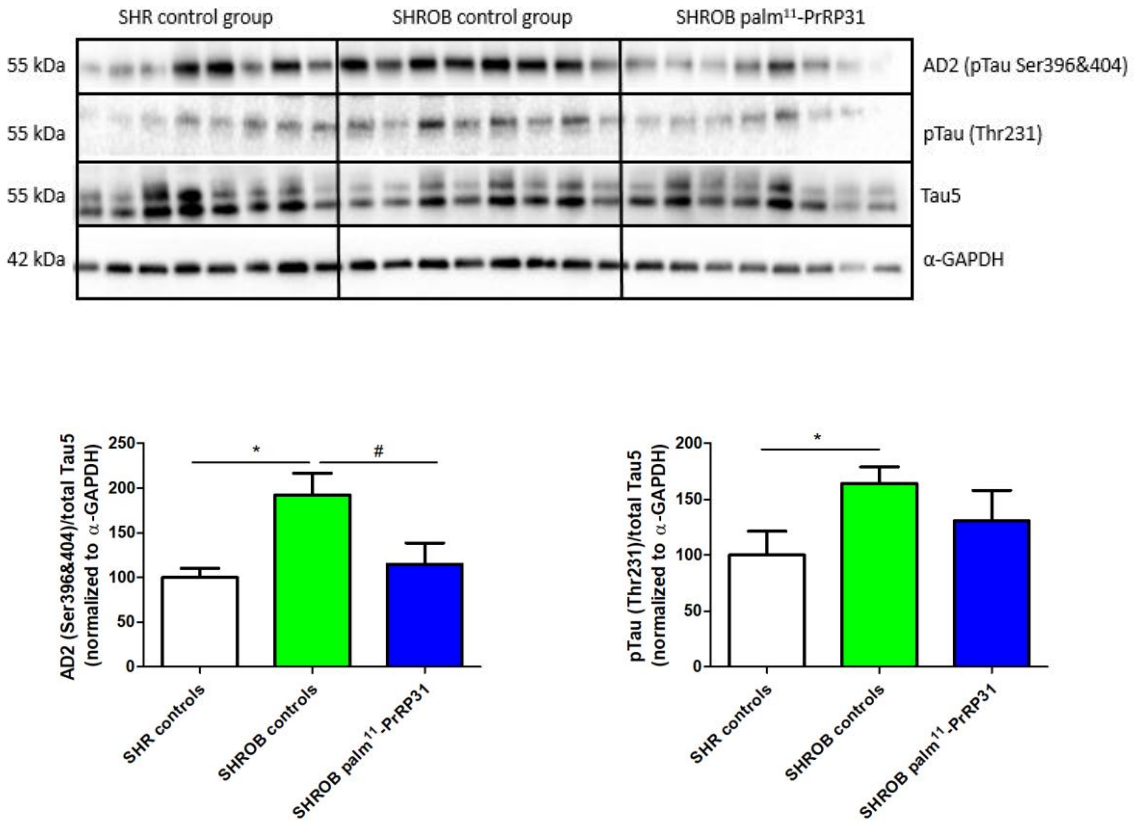

Fig. 19 Western blot analysis of Tau phosphorylation at different epitopes in hippocampi of Koletsky rats treated for 3 weeks with palm^{11}-PrRP31

*Data are mean ± SEM, n=8 rats per group. Statistical analysis was calculated by Student´s t-test. Significance is *P<0.05, #P<0.05. * SHROB controls vs SHR controls, # SHROB palm^{11}-PrRP31 vs SHROB controls.*

Markers of neurogenesis and synaptogenesis (Fig. 20) were measured in hippocampi of Koletsky rats after 3-week-long treatment with palm^{11}-PrRP31 peptide.

No significant difference was found in levels of doublecortin.

The level of PSD95, which is a marker of synaptic density, in SHROB control group was significantly increased compared to SHR control group. Compared to SHROB control group, SHROB palm^{11}-PrRP31-treated displayed significantly increased level of PSD95.

Levels of synaptophysin, which is a marker of synaptogenesis, were measured with non-significant changes.

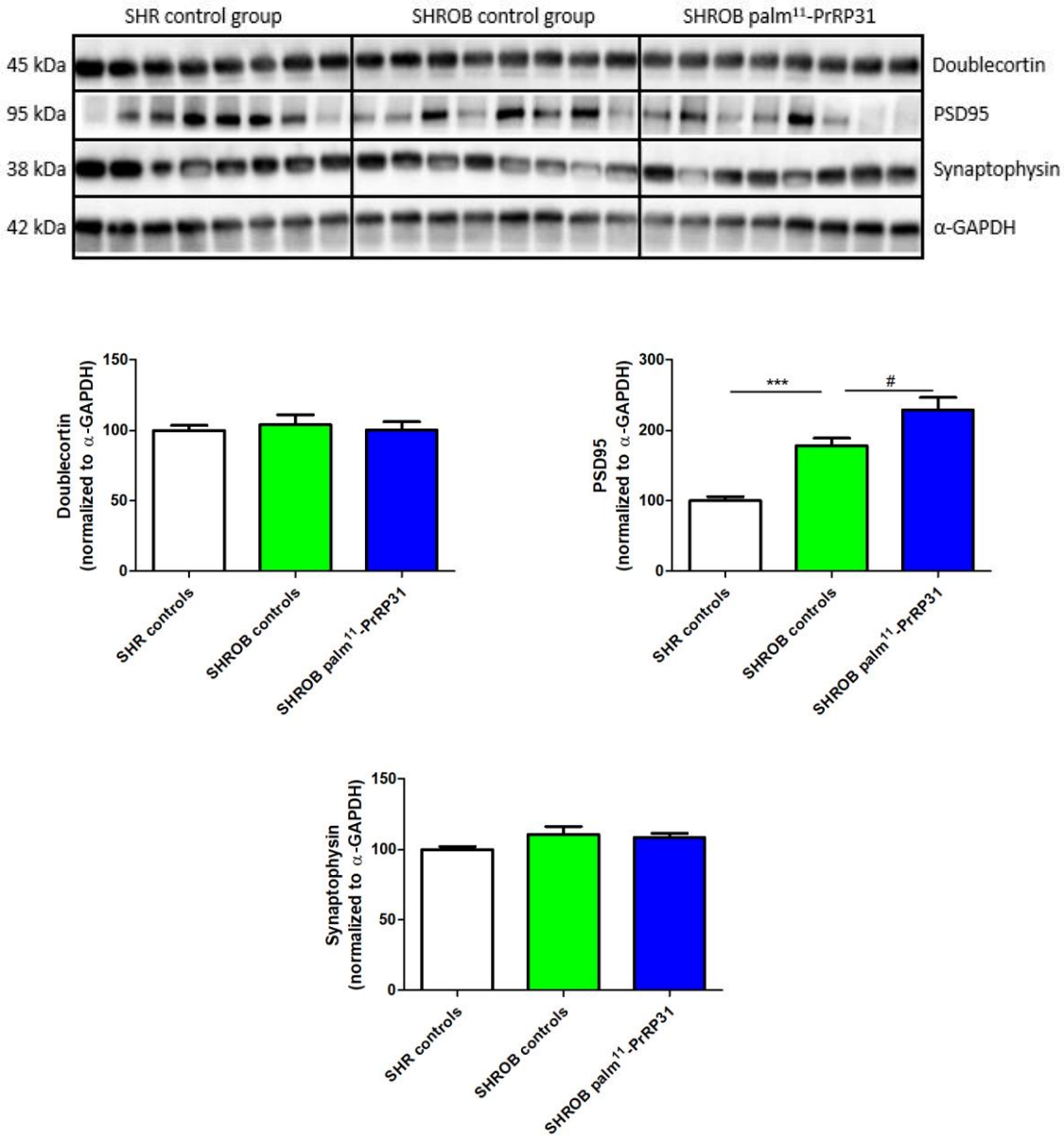

Fig. 20 Western blot analysis of markers of neurogenesis and synaptogenesis in hippocampi of Koletsky rats treated for 3 weeks with palm^{11}-PrRP31

*Data are mean ± SEM, n=8 rats per group. Statistical analysis was calculated by Student´s t-test. Significance is ***P<0.001, #P<0.05. * SHROB controls vs SHR controls, # SHROB palm^{11}-PrRP31 vs SHROB controls.*

5 DISCUSSION

AD is a chronic, progressive and neurodegenerative disease. The mechanism of AD remains still unknown. AD, as the most common type of dementia, is affecting over 50% of the population aged over 85. To date, there is no suitable AD treatment. The main risk factors is age. Recently, numerous experimental studies have shown a connection between AD development and metabolic disorders such as T2DM or obesity [67,68]. This discovery had led to intensive research. At both disorders, T2DM and AD, impaired insulin signaling was detected which could contribute to hyperphosphorylation of Tau protein. These findings have shown that anti-diabetic and/or anorexigenic peptides could have neuroprotective properties and could be used as a potential AD treatment.

In the first part of my diploma thesis, the neuroprotective properties of peptides on SH-SY5Y cells were described.

In the second part, a beneficial effect of long-term treatment with palm^{11}-PrRP31, novel analog of PrRP31, was described. We examined its effect on Tau hyperphosphorylation in THY-Tau22 mice, and in rat model of metabolic syndrome, Koletsky rats, which are likely to develop pathological Tau hyperphosphorylation according to previously mentioned risk factors of AD.

5.1 Neuroprotective properties of PrRP31, its novel palmitoylated analog palm^{11}-PrRP31 and liraglutide were proven in MG-affected SH-SY5Y cells

According to a previous study by Sharma et al. on SH-SY5Y [45], which demonstrated that drug used as a treatment for T2DM, liraglutide, has neuroprotective properties and reduces MG-induced apoptosis. Therefore we decided to analyze potential neuroprotective properties of novel PrRP31 analog palm^{11}-PrRP31.

The results presented in this diploma thesis show that liraglutide, PrRP31 and its novel lipidized analog have prophylactic neuroprotective properties against a toxic dose of MG in SH-SY5Y cells. MG as a toxic compound increases oxidative stress and interferes with energy metabolism of the cell same as it is compromised in the brain affected by AD.

Performed MTT test verified that liraglutide is able to protect SH-SY5Y cells from toxic effect of MG. Moreover, PrRP31 in concetration 10^{-5} mol·dm^{-3} and novel

analog of PrRP31, palm^{11}-PrRP31, in concentration 10^{-5} mol·dm^{-3} significantly increased cell viability in MG-stressed SH-SY5Y cells determined by the MTT test.

MG-induced cytotoxic effect was determined by measuring LDH concentration in medium. Pretreatement of SH-SY5Y cells by potentially neuroprotective peptides should protect cells from the cytotoxic effect of MG. Newly tested PrRP31 and its analog, palm^{11}-PrRP31, in both used concetrations decreased toxic effect of MG in SH.SY5Y cells in higher extension than liraglutide at concentration $1 \cdot 10^{-4}$ mol·dm^{-3}.

Thus, we have proven that tested peptides have anti-apoptotic and anti-cytotoxic effects.

5.2 Two-month-long treatment with palm^{11}-PrRP31 improved spatial memory and attenuated Tau protein hyperphosphorylation in hippocampi of THY-Tau22 mice

Similarily as in the study with MSG obese mice where palm^{1}-PrRP31 showed positive effects on the attenuation of Tau protein hyperphosphorylation [21], another analog of PrRP31, palm^{11}-PrRP31, in this study improved spatial memory tested in Y-maze and lowered Tau hyperphosphorylation in hippocampi of THY-Tau22 mice overexpressing mutant human Tau protein.

Because of the anorexigenic properties of palm^{11}-PrPR31, metabolic parameters of THY-Tau22 mice and WT control mice were measured at the end of the experiment. The treatment did not affect body weight that was rather expected as lipidized PrRP31 affects body weight of obese but not lean animals such as THY-Tau22 mice. THY-Tau22 mice had lower body weight that WT controls which was reported earlier in another study [50]. There were no significant changes in the level of glucose, leptin, insulin or WAT that were similar to those in WT control group. The 2-month-long treatment with palm^{11}-PrRP31 did not result in any significant metabolic changes in THY-Tau22 mice.

Before the beginning of the palm^{11}-PrRP31 treatment, the spatial memory was tested. In several published studies using behavioral tests, an impaired spatial memory was observed in THY-Tau22 mice. In this experiment, spatial memory was significantly impaired in 7-month-old THY-Tau22 mice compared to the control group using Y-maze. The 2-month-long palm^{11}-PrRP31 treatment resulted in improvement of spatial memory compared to the THY-Tau22 control group regarding the time spent in the

novel arm of Y-maze. The memory impairment could be caused by hyperphosphorylation of Tau protein in hippocampus, the centre of learning and memory, as can also be seen in the other mouse models of AD-like tauopathies. The memory impairment could be also caused by lowered neurogenesis and synaptic plasticity.

The 2-month-long palm^{11}-PrRP31 treatment in our study resulted in significantly decreased hyperphosphorylation of Tau protein at Thr231 epitope and non-significantly decreased at Ser202 and Thr205 epitopes. These epitopes are important in progression of AD, epitope Thr231 is the first epitope affected by AD. The lowered levels of Tau protein phosphorylation in THY-Tau22 mice treated with palm^{11}-PrRP31 positively correlate with results of spatial memory improvement observed in Y-maze. No significant changes caused by palm^{11}-PrRP31were observed in the levels of BDNF and doublecortin, both markers of neurogenesis. Non significant changes in the levels of BDNF in hippocampi of THY-Tau22 mice compared to their controls were reported in previous study [69]. Decrease in BDNF is not associated with Tau pathology. Nevertheless, a significant effect of palm^{11}-PrRP31 treatment on spatial memory and levels of Tau protein phosphorylation was observed. The results showed that palm^{11}-PrRP31 is effective on attenuation of Tau protein phosphorylation. So we can conclude that palm^{11}-PrRP31 has potential neuroprotective properties.

5.3 Three-week-long palm^{11}-PrRP31 treatment attenuated Tau protein phosphorylation in hippocampi of Koletsky (SHROB) rats

In the study on fa/fa rats, it was verified that obesity is a risk factor of impairment in insulin signaling pathway which may lead to pathological hyperphosphorylation of Tau protein [27]. Based on the effect of lipidized PrRP31 in MSG obese mice [21], insulin signaling pathway and Tau protein phosphorylation were followed in Koletsky (SHROB) rats after IP palm^{11}-PrRP31 administration, in order to find out if novel analog palm^{11}-PrRP31 has benefitial effect on possible pathological changes in insulin signaling pathway and hyperphosphorylation of Tau protein

Koletsky rat model is not a model of neurodegeneration but model of metabolic syndrome [57] since it is based on spontaneously hypertensive rats and Sprague-Dawley rats with disrupted leptin signaling similarly as in fa/fa rat model [27]. So, we hypothesized that impairment in the brain insulin signaling and following

neurodegeneration can appear with againg.

In our study, increased levels of hippocampal Tau protein phosphorylation was observed in SHROB control group compared to SHR control group. After the 3-week-long palm^{11}-PrRP31 treatment, an attenuated Tau protein hyperphosphorylation was observed in hippocampi of Koletsky rats. Significantly lower phosphorylation of Tau protein was observed at Ser396 and Ser404 epitopes. Non-significant decrease was observed at Thr231 epitope.

To determine the mechanism of palm^{11}-PrRP31 action, the most important kinases implicated in insulin signaling pathway and Tau phosphorylation were measured. The main kinase directly mediating Tau phosphorylation is GSK-3β through its Thr231 epitope. No significant changes were observed in phosphorylation of GSK-3β, neither in kinases implicated in insulin signaling pathway such as PI3K, PDK and Akt.

Another kinase which is directly affecting Tau phosphorylation is cdk-5. Significantly lowered level of cdk-5 was observed in SHROB palm^{11}-PrRP31 treated group compared to SHROB controls. This finding can explain the mechanism of attenuation of Tau phosphorylation in hippocampi of Koletsky rats.

No significant changes were found in phosphorylation of MAPK (Erk1/2) and in the level of phosphatase PP2A sub C.

Markers of neurogenensis and synaptogenesis were also examined to determine beneficial effect of palm^{11}-PrRP31. No significant changes were found in level of doublecortin, which is a marker of neurogenesis and in synaptophysin, which is a marker of synaptogenesis. Significantly increased level of PSD95, which is a protein of postsynaptic density, was observed in SHROB group treated with palm^{11}-PrRP31 compared to SHROB control rats.

According to this finding, palm^{11}-PrRP31 has beneficial effect not only on attenuation of Tau protein hyperphosphorylation, but also on postsynaptic density.

So, we can conclude that palm^{11}-PrRP31 has a benefitial effect on kinase involved in Tau phosphorylation and attenuation of Tau protein hyperphosphorylation.

6 CONCLUSIONS

In *in vitro* model of neurodegeneration caused by toxic effect of MG on SH-SY5Y cell line, tested peptides, PrRP31 and palm^{11}-PrRP31 shown neuroprotective properties manifested by increased viability. Tested peptides have anti-apoptotic effects.

Two-month long administration of palm^{11}-PrRP31 improved the short-term spatial memory of THY-Tau22 mice tested in the Y-maze and attenuated pathological hyperphosphorylation of Tau protein at different epitopes.

Three-week long administration of palm^{11}-PrRP31 benefitially effected kinase and attenuated pathological hyperphosphorylation of Tau protein. Palm^{11}-PrRP31 also benefitially altered level of marker of neurogenesis.

In conclusion, these results indicate that novel stable PrRP31 analog, palm11-PrRP31, has potential neuroprotective properties and potentially could be used in future as a sufficient treatment of neurological disorders, such as AD.

REFERENCES

1. Frisardi V, Solfrizzi V, Seripa D, *et al.* Metabolic-cognitive syndrome: a cross-talk between metabolic syndrome and Alzheimer's disease. *Ageing Res Rev* 2010; **9**: 399-417.
2. Li L, Hölscher C. Common pathological processes in Alzheimer disease and type 2 diabetes: a review. *Brain Res Rev* 2007; **56**: 384-402.
3. Knight EM, Martins IV, Gümüsgöz S, *et al.* High-fat diet-induced memory impairment in triple-transgenic Alzheimer's disease (3xTgAD) mice is independent of changes in amyloid and tau pathology. *Neurobiol Aging* 2014; **35**: 1821-1832.
4. Giordano V, Peluso G, Iannuccelli M, *et al.* Systemic and brain metabolic dysfunction as a new paradigm for approaching Alzheimer's dementia. *Neurochem Res* 2007; **32**: 555-567.
5. Schindowski K, Bretteville A, Leroy K, *et al.* Alzheimer's disease-like tau neuropathology leads to memory deficits and loss of functional synapses in a novel mutated tau transgenic mouse without any motor deficits. *Am J Pathol* 2006; **169**: 599-616.
6. Association As. 2010 Alzheimer's disease facts and figures. *Alzheimers Dement* 2010; **6**: 158-194.
7. de la Monte SM, Wands JR. Alzheimer's disease is type 3 diabetes-evidence reviewed. *J Diabetes Sci Technol* 2008; **2**: 1101-1113.
8. Hippius H, Neundörfer G. The discovery of Alzheimer's disease. *Dialogues Clin Neurosci* 2003; **5**: 101-108.
9. http://interfacegroup.ch/teaching/student-projects/amyloid-beta-dynamics-in-the-brain-computational-model-of-physiology-and-alzheimer-pathology/. Cited 31.1.2018.
10. Priller C, Bauer T, Mitteregger G, *et al.* Synapse formation and function is modulated by the amyloid precursor protein. *J Neurosci* 2006; **26**: 7212-7221.
11. Turner PR, O'Connor K, Tate WP, *et al.* Roles of amyloid precursor protein and its fragments in regulating neural activity, plasticity and memory. *Prog Neurobiol* 2003; **70**: 1-32.
12. Bamburg JR, Bloom GS. Cytoskeletal pathologies of Alzheimer disease. *Cell Motil Cytoskeleton* 2009; **66**: 635-649.
13. Chen W, Abud EA, Yeung ST, *et al.* Increased tauopathy drives microglia-mediated clearance of beta-amyloid. *Acta Neuropathol Commun* 2016; **4**: 63.
14. Gong CX, Iqbal K. Hyperphosphorylation of microtubule-associated protein tau: a promising therapeutic target for Alzheimer disease. *Curr Med Chem* 2008; **15**: 2321-2328.
15. de la Monte SM, Tong M. Brain metabolic dysfunction at the core of Alzheimer's disease. *Biochem Pharmacol* 2014; **88**: 548-559.
16. Buée L, Bussière T, Buée-Scherrer V, *et al.* Tau protein isoforms, phosphorylation and role in neurodegenerative disorders. *Brain Res Brain Res Rev* 2000; **33**: 95-130.
17. Šimić G, Babić Leko M, Wray S, *et al.* Tau Protein Hyperphosphorylation and Aggregation in Alzheimer's Disease and Other Tauopathies, and Possible Neuroprotective Strategies. *Biomolecules* 2016; **6**: 6.
18. Kimura T, Ishiguro K, Hisanaga S. Physiological and pathological

phosphorylation of tau by Cdk5. *Front Mol Neurosci* 2014; **7**: 65.
19. Kobayashi H, Saito T, Sato K, *et al.* Phosphorylation of cyclin-dependent kinase 5 (Cdk5) at Tyr-15 is inhibited by Cdk5 activators and does not contribute to the activation of Cdk5. *J Biol Chem* 2014; **289**: 19627-19636.
20. Jacobs KM, Bhave SR, Ferraro DJ, *et al.* GSK-3β: A Bifunctional Role in Cell Death Pathways. *Int J Cell Biol* 2012; **2012**: 930710.
21. Špolcová A, Mikulášková B, Holubová M, *et al.* Anorexigenic lipopeptides ameliorate central insulin signaling and attenuate tau phosphorylation in hippocampi of mice with monosodium glutamate-induced obesity. *J Alzheimers Dis* 2015; **45**: 823-835.
22. Park SA. A common pathogenic mechanism linking type-2 diabetes and Alzheimer's disease: evidence from animal models. *J Clin Neurol* 2011; **7**: 10-18.
23. Bhat RV, Budd Haeberlein SL, Avila J. Glycogen synthase kinase 3: a drug target for CNS therapies. *J Neurochem* 2004; **89**: 1313-1317.
24. Jope RS, Yuskaitis CJ, Beurel E. Glycogen synthase kinase-3 (GSK3): inflammation, diseases, and therapeutics. *Neurochem Res* 2007; **32**: 577-595.
25. Papon MA, El Khoury NB, Marcouiller F, *et al.* Deregulation of protein phosphatase 2A and hyperphosphorylation of τ protein following onset of diabetes in NOD mice. *Diabetes* 2013; **62**: 609-617.
26. Banks WA, Owen JB, Erickson MA. Insulin in the brain: there and back again. *Pharmacol Ther* 2012; **136**: 82-93.
27. Špolcová A, Mikulášková B, Kršková K, *et al.* Deficient hippocampal insulin signaling and augmented Tau phosphorylation is related to obesity- and age-induced peripheral insulin resistance: a study in Zucker rats. *BMC Neurosci* 2014; **15**: 111.
28. Lizcano JM, Alessi DR. The insulin signalling pathway. *Curr Biol* 2002; **12**: R236-238.
29. Hölscher C, Li L. New roles for insulin-like hormones in neuronal signalling and protection: new hopes for novel treatments of Alzheimer's disease? *Neurobiol Aging* 2010; **31**: 1495-1502.
30. Malm-Erjefält M, Bjørnsdottir I, Vanggaard J, *et al.* Metabolism and excretion of the once-daily human glucagon-like peptide-1 analog liraglutide in healthy male subjects and its in vitro degradation by dipeptidyl peptidase IV and neutral endopeptidase. *Drug Metab Dispos* 2010; **38**: 1944-1953.
31. Ladenheim EE. Liraglutide and obesity: a review of the data so far. *Drug Des Devel Ther* 2015; **9**: 1867-1875.
32. McClean PL, Parthsarathy V, Faivre E, *et al.* The diabetes drug liraglutide prevents degenerative processes in a mouse model of Alzheimer's disease. *J Neurosci* 2011; **31**: 6587-6594.
33. Maletínská L, Nagelová V, Tichá A, *et al.* Novel lipidized analogs of prolactin-releasing peptide have prolonged half-lives and exert anti-obesity effects after peripheral administration. *Int J Obes (Lond)* 2015; **39**: 986-993.
34. Gu W, Geddes BJ, Zhang C, *et al.* The prolactin-releasing peptide receptor (GPR10) regulates body weight homeostasis in mice. *J Mol Neurosci* 2004; **22**: 93-103.
35. Hinuma S, Habata Y, Fujii R, *et al.* A prolactin-releasing peptide in the brain. *Nature* 1998; **393**: 272-276.

36. Onaka T, Takayanagi Y, Leng G. Metabolic and stress-related roles of prolactin-releasing peptide. *Trends Endocrinol Metab* 2010; **21**: 287-293.
37. Maixnerová J, Špolcová A, Pýchová M, *et al.* Characterization of prolactin-releasing peptide: binding, signaling and hormone secretion in rodent pituitary cell lines endogenously expressing its receptor. *Peptides* 2011; **32**: 811-817.
38. Lagerström MC, Fredriksson R, Bjarnadóttir TK, *et al.* Origin of the prolactin-releasing hormone (PRLH) receptors: evidence of coevolution between PRLH and a redundant neuropeptide Y receptor during vertebrate evolution. *Genomics* 2005; **85**: 688-703.
39. Dodd GT, Luckman SM. Physiological Roles of GPR10 and PrRP Signaling. *Front Endocrinol (Lausanne)* 2013; **4**: 20.
40. Fukusumi S, Fujii R, Hinuma S. Recent advances in mammalian RFamide peptides: the discovery and functional analyses of PrRP, RFRPs and QRFP. *Peptides* 2006; **27**: 1073-1086.
41. Prazienkova V, Ticha A, Blechova M, *et al.* Pharmacological characterization of lipidized analogs of prolactin-releasing peptide with a modified C- terminal aromatic ring. *J Physiol Pharmacol* 2016; **67**: 121-128.
42. Lawrence CB, Liu YL, Stock MJ, *et al.* Anorectic actions of prolactin-releasing peptide are mediated by corticotropin-releasing hormone receptors. *Am J Physiol Regul Integr Comp Physiol* 2004; **286**: R101-107.
43. Bjursell M, Lennerås M, Göransson M, *et al.* GPR10 deficiency in mice results in altered energy expenditure and obesity. *Biochem Biophys Res Commun* 2007; **363**: 633-638.
44. Pražienková V, Holubová M, Pelantová H, *et al.* Impact of novel palmitoylated prolactin-releasing peptide analogs on metabolic changes in mice with diet-induced obesity. *PLoS One* 2017; **12**: e0183449.
45. Sharma MK, Jalewa J, Hölscher C. Neuroprotective and anti-apoptotic effects of liraglutide on SH-SY5Y cells exposed to methylglyoxal stress. *J Neurochem* 2014; **128**: 459-471.
46. Shipley MM, Mangold CA, Kuny CV, *et al.* Differentiated Human SH-SY5Y Cells Provide a Reductionist Model of Herpes Simplex Virus 1 Neurotropism. *J Virol* 2017; **91**.
47. Greene LA, Tischler AS. Establishment of a noradrenergic clonal line of rat adrenal pheochromocytoma cells which respond to nerve growth factor. *Proc Natl Acad Sci U S A* 1976; **73**: 2424-2428.
48. Haile Y, Fu W, Shi B, *et al.* Characterization of the NT2-derived neuronal and astrocytic cell lines as alternative in vitro models for primary human neurons and astrocytes. *J Neurosci Res* 2014; **92**: 1187-1198.
49. Jankowsky JL, Fadale DJ, Anderson J, *et al.* Mutant presenilins specifically elevate the levels of the 42 residue beta-amyloid peptide in vivo: evidence for augmentation of a 42-specific gamma secretase. *Hum Mol Genet* 2004; **13**: 159-170.
50. Leboucher A, Laurent C, Fernandez-Gomez FJ, *et al.* Detrimental effects of diet-induced obesity on τ pathology are independent of insulin resistance in τ transgenic mice. *Diabetes* 2013; **62**: 1681-1688.
51. Van der Jeugd A, Blum D, Raison S, *et al.* Observations in THY-Tau22 mice that resemble behavioral and psychological signs and symptoms of dementia. *Behav Brain Res* 2013; **242**: 34-39.

52. Oddo S, Caccamo A, Shepherd JD, *et al.* Triple-transgenic model of Alzheimer's disease with plaques and tangles: intracellular Abeta and synaptic dysfunction. *Neuron* 2003; **39**: 409-421.
53. Ramos-Rodriguez JJ, Ortiz O, Jimenez-Palomares M, *et al.* Differential central pathology and cognitive impairment in pre-diabetic and diabetic mice. *Psychoneuroendocrinology* 2013; **38**: 2462-2475.
54. Olney JW. Brain lesions, obesity, and other disturbances in mice treated with monosodium glutamate. *Science* 1969; **164**: 719-721.
55. Zucker LM, Antoniades HN. Insulin and obesity in the Zucker genetically obese rat "fatty". *Endocrinology* 1972; **90**: 1320-1330.
56. Zhao M, Li Y, Wang J, *et al.* Azilsartan treatment improves insulin sensitivity in obese spontaneously hypertensive Koletsky rats. *Diabetes Obes Metab* 2011; **13**: 1123-1129.
57. Koletsky S. Pathologic findings and laboratory data in a new strain of obese hypertensive rats. *Am J Pathol* 1975; **80**: 129-142.
58. Wei Z, Chen XC, Song Y, *et al.* Amyloid β Protein Aggravates Neuronal Senescence and Cognitive Deficits in 5XFAD Mouse Model of Alzheimer's Disease. *Chin Med J (Engl)* 2016; **129**: 1835-1844.
59. http://med.stanford.edu/sbfnl/services/bm/lm/y-maze.html. Cited 6.3.2017.
60. Vorhees CV, Williams MT. Morris water maze: procedures for assessing spatial and related forms of learning and memory. *Nat Protoc* 2006; **1**: 848-858.
61. Reiserer RS, Harrison FE, Syverud DC, *et al.* Impaired spatial learning in the APPSwe + PSEN1DeltaE9 bigenic mouse model of Alzheimer's disease. *Genes Brain Behav* 2007; **6**: 54-65.
62. Seibenhener ML, Wooten MC. Use of the Open Field Maze to measure locomotor and anxiety-like behavior in mice. *J Vis Exp* 2015: e52434.
63. Tajes M, Eraso-Pichot A, Rubio-Moscardó F, *et al.* Methylglyoxal reduces mitochondrial potential and activates Bax and caspase-3 in neurons: Implications for Alzheimer's disease. *Neurosci Lett* 2014; **580**: 78-82.
64. https://worldwide.promega.com/products/cell-health-assays/cell-viability-and-cytotoxicity-assays/cytotox-96-non_radioactive-cytotoxicity-assay/?catNum=G1780. Cited 10.1.2018.
65. Popelová A, Pražienková V, Neprašová B, *et al.* Novel Lipidized Analog of Prolactin-Releasing Peptide Improves Memory Impairment and Attenuates Hyperphosphorylation of Tau Protein in a Mouse Model of Tauopathy. *J Alzheimers Dis* 2018; **62**: 1725-1736.
66. Mikulášková B, Holubová M, Pražienková V, *et al.* Lipidized prolactin-releasing peptide improved glucose tolerance in metabolic syndrome: Koletsky and spontaneously hypertensive rat study. *Nutr Diabetes* 2018; **8**: 5.
67. Hassing LB, Dahl AK, Thorvaldsson V, *et al.* Overweight in midlife and risk of dementia: a 40-year follow-up study. *Int J Obes (Lond)* 2009; **33**: 893-898.
68. Schrijvers EM, Witteman JC, Sijbrands EJ, *et al.* Insulin metabolism and the risk of Alzheimer disease: the Rotterdam Study. *Neurology* 2010; **75**: 1982-1987.
69. Burnouf S, Belarbi K, Troquier L, *et al.* Hippocampal BDNF expression in a tau transgenic mouse model. *Curr Alzheimer Res* 2012; **9**: 406-410.